Optimal Wireless Resource Allocation for Scalable Video Transmission over Cognitive Radio Networks

Η ΜΕΤΑΠΤΥΧΙΑΚΗ ΕΡΓΑΣΙΑ ΕΞΕΙΔΙΚΕΥΣΗΣ

υποβάλλεται στην

ορισθείσα από την Γενική Συνέλευση Ειδικής Σύνθεσης

του Τμήματος Μηχανικών Η/Υ και Πληροφορικής
Εξεταστική Επιτροπή

από τον

Αλέξανδρο Φραγκούλη

ως μέρος των Υποχρεώσεων για τη λήψη του

ΜΕΤΑΠΤΥΧΙΑΚΟΥ ΔΙΠΛΩΜΑΤΟΣ ΣΤΗΝ ΠΛΗΡΟΦΟΡΙΚΗ

ΜΕ ΕΞΕΙΔΙΚΕΥΣΗ

ΣΤΙΣ ΤΕΧΝΟΛΟΓΙΕΣ-ΕΦΑΡΜΟΓΕΣ

Απρίλιος 2014

DEDICATION

To my beloved family..

ACKNOWLEDGEMENTS

I would like to express my deep gratitude to my supervisor Associate Professor Lisimachos Paul Kondi for his patient guidance, continuous assistance and encouragement for the completion of this research work. I would also like to express my great appreciation to Assistant Professor Konstantinos Parsopoulos for his important contribution, valuable advice and insightful critiques. Special thanks to PhD candidates Angeliki Katsenou and Katerina Pandremmenou for offering their eager support on many technical matters.

However, this thesis would have never been completed without the constant encouragement and invaluable support of my mother and my sister. I would like to express my deepest love and gratitude to them.

TABLE OF CONTENTS

LIST OF FIGURES

LIST OF TABLES

ABSTRACT

Alexandros C. Fragkoulis. MSc, Department of Computer Science and Engineering, University of Ioannina, Greece. April, 2014. Optimal Wireless Resource Allocation for Scalable Video Transmission over Cognitive Radio Networks. Thesis Supervisor: Lisimachos Paul Kondi.

The increasing number of wireless multimedia networks and high-rate multimedia applications, has caused an electromagnetic spectrum congestion. Cognitive Radio is a promising technology that confronts the problem of spectrum scarcity, caused by the current spectrum licensing policies. CR systems are intelligent wireless communication systems which are aware of their environment and support reliable communication by efficiently utilizing the available electromagnetic spectrum.

In the present thesis, we propose a method for the fair and efficient allocation of wireless resources over a cognitive radio system network, to transmit multiple scalable video streams to multiple users. We use a game-theoretic Nash Bargaining Solution (NBS) framework to ensure that each user receives the minimum video quality requirements, while maintaining fairness over the cognitive radio system. Moreover, we implement a state-of-the-art approach, based on maximizing the aggregate visual quality of cognitive users, to compare and evaluate the results.

Given the dynamic spectrum management of CR systems, both methods exploit the dynamic architecture of the Scalable Video Coding extension of the H.264 standard, along with the diversity that Orthogonal Frequency Division Multiple Access (OFDMA) networks provide. The SVC extension of the H.264 standard provides desirable features for many multimedia applications, as it enables the adaptation to channel conditions and fulfils different transmission requirements. For further communication improvement, we use multiple antennas at the cognitive base station (Multiple-Input-Single-Output antenna system).

With these system settings, for each method an optimization problem is formulated. The objective in the proposed method is the maximization of the Nash product, while in the second method the objective is the maximization of the aggregate visual quality. In both cases the minimization of resources waste is imposed as an optimization criterion, to avoid allocating more resources than are necessary to attain a specific visual quality. Each problem is solved by a Swarm Intelligence optimizer, namely Particle Swarm Optimization. Due to the high dimensionality of the problem, we also introduce

a dimension-reduction technique.

The notions of fairness and efficiency are quantified by employing two metrics, namely the Jain's Index (fairness) and Aggregate Utility Index (efficiency). The performance of each method in terms of fairness and efficiency is illustrated through comparisons with the Peak Signal-to-Noise Ratio (PSNR) each cognitive user receives, which is a measure of visual quality.

We conducted experiments to investigate two cases. The first case regarded the transmission of a single video sequence to all cognitive users, whilst in the second case, multiple video sequences were transmitted. The results of the conducted experiments exhibited the superiority of the proposed method against the aggregate visual quality method in terms of fairness. A slightly better performance of the second method in terms of efficiency was also reported, as it was expected, since this method defines optimality in terms of the aggregated visual quality of the received video sequences of all users.

ΕΚΤΕΤΑΜΕΝΗ ΠΕΡΙΛΗΨΗ ΣΤΑ ΕΛΛΗΝΙΚΑ

Αλέξανδρος Φραγκούλης του Χαριλάου και της Ειρήνης. MSc, Τμήμα Μηχανικών Η/Υ και Πληροφορικής, Πανεπιστήμιο Ιωαννίνων, Απρίλιος, 2014. Βέλτιστη κατανομή ασύρματων πόρων για τη μετάδοση κλιμακωτών εικονοσειρών σε γνωστικά δίκτυα ραδιεπικοινωνιών. Επιβλέποντας: Λυσίμαχος Παύλος Κόντης.

Ο συνεχώς αυξανόμενος αριθμός των ασύρματων πολυμεσικών δικτύων και των πολυμεσικών εφαρμογών που απαιτούν υψηλούς ρυθμούς μετάδοσης πληροφορίας, έχει προκαλέσει τη συμφόρηση του ηλεκτρομαγνητικού φάσματος. Τα γνωστικά συστήματα ραδιοεπικοινωνιών (Cognitive Radio systems) είναι μια πολλά υποσχόμενη τεχνολογία, η οποία επιχειρεί να αντιμετωπίσει το πρόβλημα της έλλειψης διαθέσιμου φάσματος που προκαλείται από τις τρέχουσες πολιτικές διάθεσής του. Πρόκειται για ευφυή συστήματα ασύρματων επικοινωνιών, τα οποία έχουν γνώση του περιβάλλοντός τους και υποστηρίζουν αξιόπιστες επικοινωνίες, αξιοποιώντας κατάλληλα το διαθέσιμο ηλεκτρομαγνητικό φάσμα.

Στην παρούσα διατριβή, προτείνουμε μία μέθοδο για την δίκαιη και αποδοτική κατανομή των ασύρματων πόρων σε δίκτυα γνωστικών ραδιοεπικοινωνιών, για την μετάδοση πολλαπλών κλιμακωτών εικονοσειρών σε πολλαπλούς χρήστες. Χρησιμοποιούμε ένα πλαίσιο βασισμένο στη Θεωρία Παιγνίων και συγκεκριμένα στη Λύση Διαπραγμάτευσης του Nash, έτσι ώστε να διασφαλίζεται ότι κάθε χρήστης θα λαμβάνει το ελάχιστο απαιτούμενο επίπεδο ποιότητας, ενώ παράλληλα θα εξασφαλίζεται η δίκαιη αντιμετώπιση των χρηστών του γνωστικού συστήματος. Επιπλέον, υλοποιούμε μια προσέγγιση που έχει ερευνηθεί πρόσφατα, η οποία βασίζεται στη μεγιστοποίηση της συνολικής οπτικής ποιότητας των χρηστών του γνωστικού συστήματος, για να συγκρίνουμε και να αξιολογήσουμε τα αποτελέσματα.

Δεδομένης της δυναμικής διαχείρισης του φάσματος που παρέχουν τα γνωστικά συστήματα, οι δύο μέθοδοι που παρουσιάζουμε εκμεταλλεύονται τη δυναμική αρχιτεκτονική της επέκτασης Scalable Video Coding (SVC) του πρότυπου H.264, παράλληλα με τα πλεονεκτήματα που παρέχουν τα δίκτυα Πολλαπλής Πρόσβασης με Ορθογωνική Διαίρεση Συχνότητας (Orthogonal Frequency Division Multiple Access-OFDMA). Η SVC επέκταση του προτύπου H.264 παρέχει επιθυμητά χαρακτηριστικά για πολλές πολυμεσικές εφαρμογές, καθώς προσφέρει τη δυνατότητα της προσαρμογής στις εκάστοτε συνθήκες του καναλιού μετάδοσης και την ικανοποίηση διαφορετικών απαιτήσεων μετάδοσης. Για περαιτέρω βελτίωση των συνθηκών επικοινωνίας, χρησιμοποιούμε πολλαπλές κεραίες στο γνωστικό σταθμό βάσης (σύστημα κεραιών Multiple-Input-Single-Output).

Χρησιμοποιώντας αυτή τη διαμόρφωση συστήματος, για κάθε μέθοδο διατυπώνεται από

ένα πρόβλημα βελτιστοποίησης. Ο στόχος στην προτεινόμενη μέθοδο είναι η μεγιστοποίηση του γινόμενου Nash, ενώ στη δεύτερη μέθοδο είναι η μεγιστοποίηση της συνολικής οπτικής ποιότητας των χρηστών του γνωστικού δικτύου. Και στις δύο περιπτώσεις, λαμβάνεται υπόψη ως κριτήριο βελτιστοποίησης και η ελαχιστοποίηση της σπατάλης ασύρματων πόρων, έτσι ώστε να αποφεύγεται η κατανομή και η χρησιμοποίηση περισσότερων πόρων από αυτούς που απαιτούνται για να επιτυγχάνεται μια δεδομένη οπτική ποιότητα. Κάθε πρόβλημα βελτιστοποίησης λύνεται με τη βοήθεια μιας μεθόδου βελτιστοποίησης Νοημοσύνης Σμήνους (Swarm Intelligence), η οποία ονομάζεται μέθοδος Βελτιστοποίηση Σμήνους Σωματιδίων (Particle Swarm Optimization-PSO). Λόγω της υψηλής διάστασης του προβλήματος, εισάγαμε και χρησιμοποιήσαμε μια τεχνική μείωσης διάστασης.

Οι έννοιες της δικαιοσύνης και της αποδοτικότητας ποσοτικοποιήθηκαν χρησιμοποιώντας δύο μετρικές, τον Δείκτη του Jain (Jain's Index) και τον Δείκτη Συνολικής Ωφέλειας (Aggregate Utility Index), αντίστοιχα. Οι επιδόσεις κάθε μεθόδου ως προς τη δικαιοσύνη και την αποδοτικότητα παρουσιάζονται μέσω συγκρίσεων του Σηματοθορυβικού λόγου Κορυφής (Peak Signal-to-Noise Ratio) που λαμβάνει κάθε χρήστης, ο οποίος λόγος αποτελεί μέτρο της οπτικής ποιότητας.

Πραγματοποιήσαμε πειράματα για να διερευνήσουμε δύο περιπτώσεις: η πρώτη περίπτωση αφορούσε τη μετάδοση μοναδικής εικονοσειράς, ενώ η δεύτερη τη μετάδοση πολλαπλών εικονοσειρών. Τα αποτελέσματα των πειραμάτων επέδειξαν την ανωτερότητα της προτεινόμενης μεθόδου σε σχέση με τη μέθοδο συνολικής οπτικής ποιότητας ως προς τη δικαιοσύνη. Η δεύτερη μέθοδος επίδειξε ελαφρά καλύτερες επιδόσεις ως προς την αποδοτικότητα, όπως ήταν αναμενόμενο, δεδομένου ότι, ως προσέγγιση βελτιστοποίησης, τέθηκε η μεγιστοποίηση της συνολικής οπτικής ποιότητας, άρα και αποδοτικότητας, των χρηστών.

CHAPTER 1

INTRODUCTION

1.1 Motivation

Over the recent years, the number of applications related to wireless multimedia broadcasting has been increasing at a remarkable pace, illustrating the growing demand for wireless communications. This fact has been spurred by the emergence of broadband wireless services, combined with the great advances in video compression technologies. The rapid development of wireless telecommunications has led to the efficiency enhancement of various video communication services such as video conferencing, Video-On-Demand and IPTV. Many state-of-the-art wireless multimedia network system frameworks have been employed to implement surveillance, monitoring and gaming applications.

All those high rate services require effective and efficient utilization of the electromagnetic spectrum. The increasing number of wireless multimedia networks has caused a congestion of the electromagnetic spectrum. In 2002, The Spectrum Task Force was established to assist the Federal Communications Commission in defining the changes in spectrum policy that would increase the efficiency of the radio spectrum. Even though several bands were expanded, those bands were assigned exclusively to specific primary users, even for the time frame that they did not utilize them. The problem of spectrum scarcity caused by the current spectrum allocation policies have become a barrier for those high rate services. Another significant issue is the way the wireless resources are utilized. It is of great importance for the modern wireless multimedia broadcasting applications to maximize the throughtput to multiple users, while minimizing the resources waste, as the surplus can be assigned to other simultaneous transmission tasks.

1.2 Thesis Scope

In this thesis, a method for fair and efficient allocation of wireless resources over a *cognitive radio system* network, to transmit multiple scalable video streams to multiple users, is proposed. *Cognitive Radio (CR)* systems have proved to be a remarkable solution to the spectrum scarcity problem described above. CR systems are intelligent wireless communication systems which are aware of their environment and support reliable communication by efficiently utilizing the available electromagnetic spectrum. The *spectrum holes* that are unoccupied by a primary user are exploited and the available bands of frequencies are assigned to secondary communications to be used without interfering to the primary communications [1]. In addition to that, we employ a *Multiple-Input-Multiple Output (MIMO)* antenna system at the CR network. MIMO antenna systems perform much better than Single-Input-Single-Output systems in multimedia transmission. They employ beamforming techniques and, as a result, the secondary users' received signal gain is increased and the interferences to primary users are significantly reduced [2]. However, the benefits from MIMO systems come at the cost of hardware and computational complexity increase and the requirement of complete channel state information (CSI) at the transmitter. Recent works, though, have demonstrated that even if the full CSI is not available, antenna selection in MIMO systems is a promising technology offering reduced cost and complexity [3]. In such channel conditions described above, Orthogonal Frequency Division Multiple Access (OFDMA) is proposed, as it can deal with multipath interference with more robustness and can achieve a higher MIMO spectral efficiency [4].

Scalable Video Coding has been considered in recent works as a highly attractive solution to the challenges posed by the requirements of CR systems. Due to the changing channel conditions and the varying bandwidth availability of our system model, the dynamic nature of the SVC extension of the H.264 standard provides the system with the ability to adjust to the fluctuations and enhance the Quality of Service (QoS) for each user. SVC provides temporal, spatial and quality scalability. Quality scalability empowers transporting complementary data in different layers in order to produce videos with distinct quality levels. In this work, we exploit the quality scalability modality and MGS coding mode.

In recent years, CR systems have been widely used as system models to related works. First of all, in [5], the novel functionalities and current research challenges of the cognitive networks are explained in detail, while in [6], the problem of robust downlink beamforming design in a multiuser Multiple-Input Single-Output (MISO) Cognitive Radio Network in which multiple Primary Users coexist with multiple Secondary Users, is addressed. In [7], scalable video multicast in emerging CR networks is investigated; a sequential fixing algorithm and a greedy algorithm are proposed, to solve a mixed integer nonlinear programming (MINLP) problem. In [8], CGS and MGS modes are considered for allocating resources among secondary users, defining optimality in terms of the aggregate visual quality of the received video sequences. The problem is being solved using discrete programming methods. Moreover, a Nash Bargaining Solution (NBS) framework is employed

for fair power allocation among the users of a CR Orthogonal Frequency Division Multiple Access (OFDMA) system in [9]. Optimal power and bandwidth allocation is also studied in [10], where the multicast groups of secondary users use Orthogonal Frequency Division Multiplexing (OFDM). Additionally, a multiuser OFDM subcarrier, bit and power allocation algorithm to minimize the total transmit power is proposed in [11]. In [12], Fountain codes are employed to compensate for data loss caused by the primary transmission and in [13], resource management for scalable video transmission over a cognitive radio is considered, using *Time Division Multiple Access (TDMA)* method, allowing several users to share the same frequency channel by dividing the signal into different time slots. The merits of OFDM for a CR system are discussed in [14], CR systems and their requirements of the physical layer are described and OFDM technique is investigated as a candidate transmission technology for CR. A CR system utilizing OFDM is also described in [15].

In the present work, we consider the transmission of MGS video streams over a downlink cognitive radio system. We propose *Orthogonal Frequency Division Multiple Access (OFDMA)* as modulation scheme and multiple transmit antennas are used at the cognitive base station to reduce the outage probability of secondary users [8]. We formulate the problem of optimally allocating the system resources, specifically the subcarriers and the antennas, among the secondary users, with respect to fairness and efficiency objectives. Fairness is defined as the minimization of video quality deviation among users who subscribe the same Quality of Service [24]. Efficiency is defined as the maximization of the aggregate visual quality the secondary users achieve. Based on those objectives, we present two methods. In the first method, a *Nash Bargaining Solution (NBS)* framework is presented. We formulate an optimization problem with the purpose of achieving this NBS, while minimizing the unnecessary resources utilization. The second method considers the aggregate visual quality as optimality measure. In this case, the objective of the resource allocation is to maximize the aggregate *Peak Signal-to-Noise Ratio (PSNR)* of received video sequences, avoiding allocating more resources than are necessary to attain a given visual quality. To define the solutions for the formulated problems, we use a swarm intelligence optimization method, the *Particle Swarm Optimization (PSO)* [25]. Because of the high complexity of the formulated objective function, we reduce its dimension with algorithms implemented based on the system's structure.

1.3   Thesis Outline

The thesis is organized as follows:

Section 2 presents the system model features and essential background knowledge about Cognitive Radio systems, MIMO systems, Orthogonal Frequency Division Multiplexing and the Video Coding scheme.

In Section 3, we describe the proposed method, the aggregate visual quality method and their allocation frameworks along with the definition of the objective functions to be optimized.

In Section 4, we present the experiments' settings and simulation results and finally the thesis concludes in Section 5.

CHAPTER 2

BACKGROUND KNOWLEDGE

2.1 Cognitive Radio Systems

The term Cognitive Radio was first introduced by Joseph Mitola. CR systems have been proposed to exploit the existence of the spectrum holes and promote the efficient use of the spectrum. In 2005, Simon Haykin defined the cognitive radio as an intelligent wireless communication system that is aware of its environment, learns from it and adapts its internal states to statistical variations in the incoming RF stimuli by making corresponding changes in specific operating parameters (transmit power, frequency, modulation schemes) in real-time, with two primary objectives in mind: The highly reliable communication and the efficient utilization of the spectrum [1]. The changes performed in the parameters are used for future decisions. A cognitive radio depends on a platform known as *Software Defined Radio (SDR)* for the functionality of the network and the modification of the system parameters.

2.1.1 Physical Architecture of a Cognitive Radio System

A basic physical architecture of a CR system is shown in Fig. 2.1. The transceiver consists of the radio front-end and the baseband processing unit. The RF front-end is responsible for the amplification of the received signal, the mixing and finally the A/D
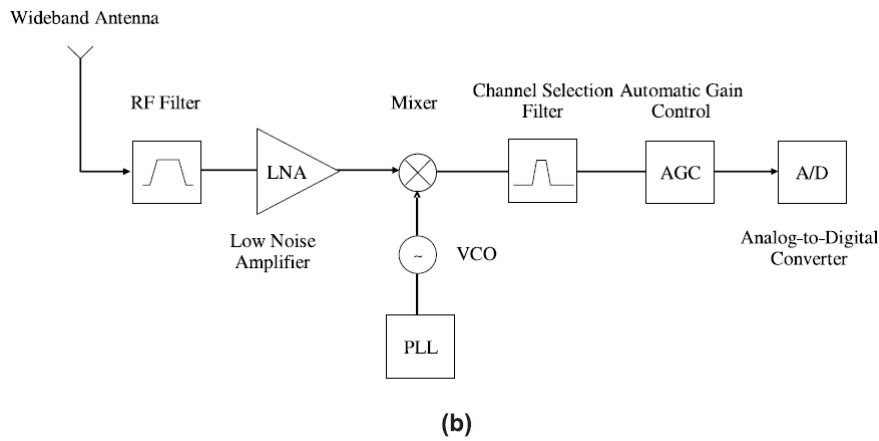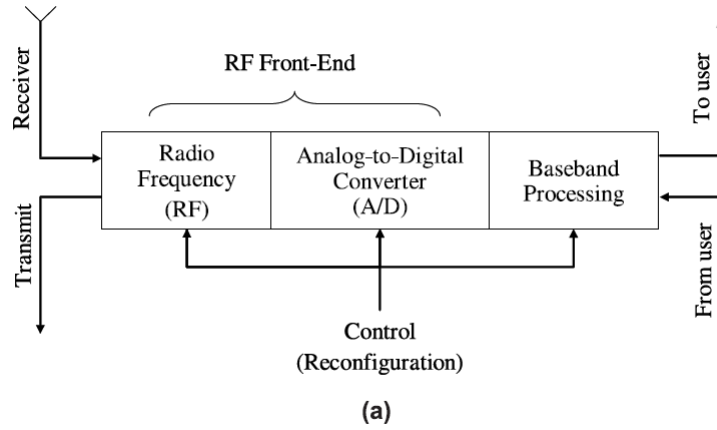
Figure 2.1: (a) Cognitive radio transceiver and (b) wideband RF front end architecture [5].

conversion. In the baseband processing unit, the signal is modulated/demodulated and encoded/decoded.

The RF front-end consists of

- a RF filter, which selects the desired band by filtering the received signal,

- a Low noise amplifier (LNA), for the amplification of the desired signal while minimizing the noise effect,

- a Mixer, in which the received signal is mixed with locally generated RF frequency and converted to the baseband or the intermediate frequency (IF),

- a Voltage-controlled oscillator (VCO), which generates a signal at a specific frequency for a voltage to mix with the received amplified signal,

- a Phase locked loop (PLL), which ensures that the frequency of the signal does not change,

- the Channel Selection Filter, which is used to select the desired channel,

- the Automatic Gain Control (AGC), to maintain the gain of an amplifier constant through the wide range of input signal levels. [5]

2.1.2 Cognitive Cycle
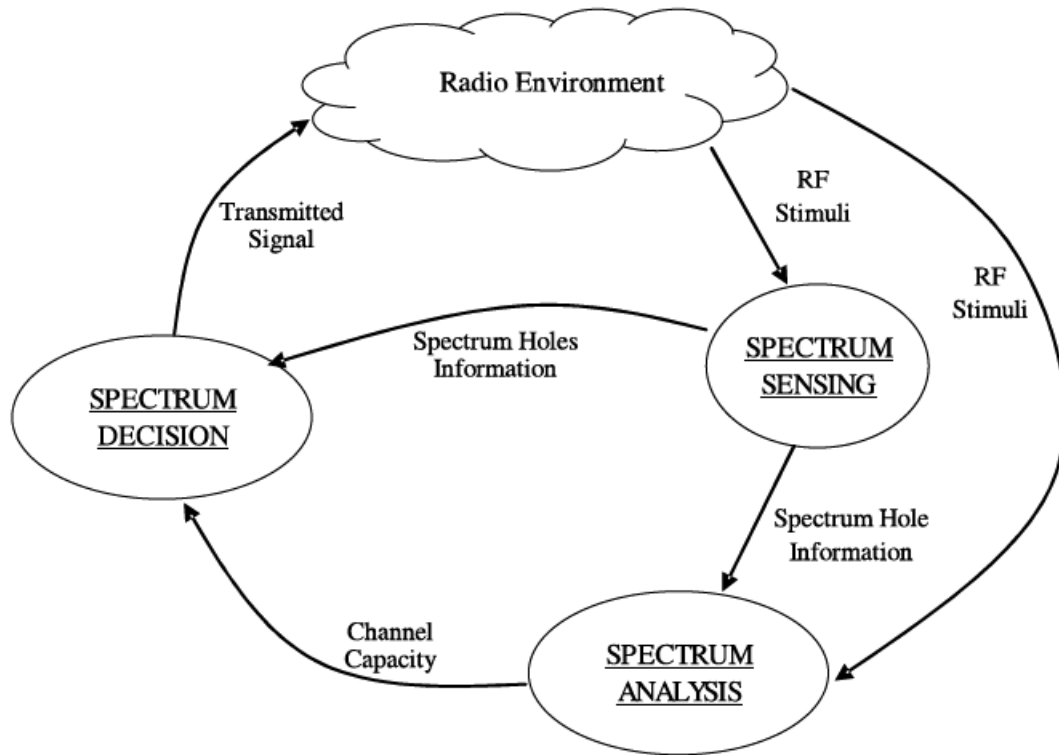
Figure 2.2: Basic Cognitive Cycle [5]

The basic cognitive cycle for a cognitive radio network is depicted in Fig. 2.2. The receiver is responsible for performing spectrum sensing and analysis before the transmission. In the receiver, the detection of spectrum holes is carried out, along with estimation of Channel State Information (CSI) and the prediction of channel capacity to be used by the transmitter. The transmitter controls the transmit-power, the data rate and/or the modulation scheme, so that the interference to the primary users of the network does not exceed specific levels.

The spectrum sensing involves the detection of spectrum bands which are unoccupied by primary users and assign them to secondary users, as long as there is no harmful interference to the primary users. It is one of the most important procedures in CR networks. Then, the results of the spectrum sensing are estimated and assessed by the spectrum analysis procedure. Finally, the parameters of the cognitive radio are defined in the spectrum decision phase and the appropriate band is selected based on the user requirements.

2.1.3   Cognitive Networks Reconfigurability

The cognitive systems have the capability of adjusting their operating parameters for the transmission on the fly without any hardware components modification. This feature is called *Reconfigurability*. The operating parameters employed by the cognitive radio systems can be altered not only at the beginning of a transmission but also during the transmission. Several of them are presented below:

- *Operating frequency*: Based on the information about the radio environment, the appropriate operating frequency is selected dynamically for the optimal output.

- *Modulation*: The modulation scheme used by the cognitive system can be determined according to the user requirements and the channel conditions. Depending on each application's bit error rate requirement, the suitable modulation scheme is enabled.

- *Transmission power*: Power control enables dynamic transmission power configuration within the power constraints. If no high power operation is necessary, the transmitter power is reduced to allow more users access the spectrum and minimize the interference.

- *Communication technology*: A cognitive radio systems provides interoperability between different telecommunication systems.

2.1.4   The Cognitive Network architecture

The Cognitive Network architecture is depicted in Fig 2.3 [5]

The components of a Cognitive network can be classified into two groups: The *Primary Network* and the *Secondary Network*. The basic elements of the primary and secondary networks are the following:

- Primary Network: This network has an exclusive right to a certain spectrum band. It consists of:

  - *Primary Users (PU)*: Primary Users (or licensed users) have a license to operate in a specific spectrum band. This access can be controlled exclusively by the primary base-station and should not be affected by the operations of any other secondary user.

  - *Primary Base-Station*: Primary base-station is a network component that has spectrum license such as the base-station transceiver system in a cellular system. The primary base-station does not have any cognitive capability for sharing spectrum with secondary users.

- Secondary Network: The secondary network (or cognitive radio network, unlicensed network) has not be granted with a license to operate in a specific spectrum band.
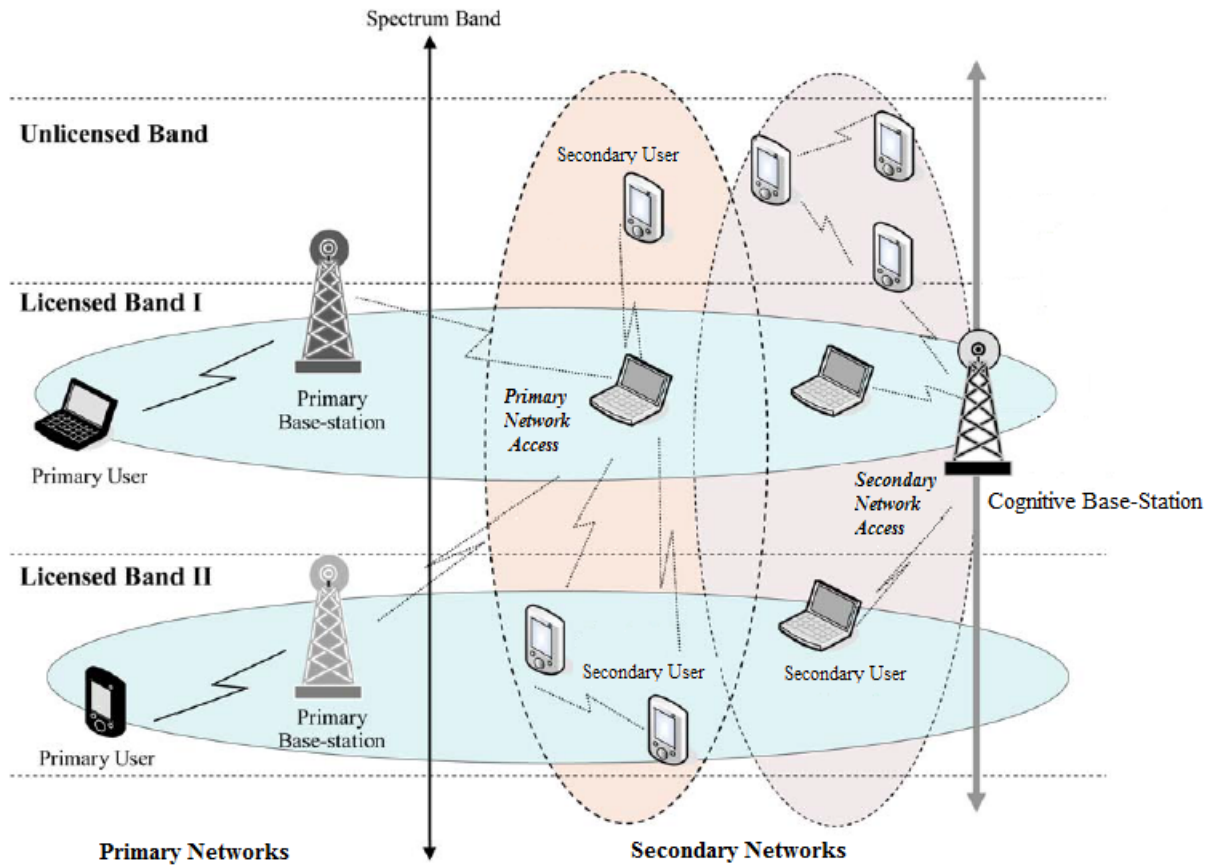
Figure 2.3: Cognitive Network architecture

The access to spectrum is opportunistic. The components of a Secondary Network are the following:

- *Secondary Users*: Secondary users (or unlicensed users), have no spectrum license and as a result any operation they perform presupposes licensed spectrum band sharing.

- *Secondary Base-Station*: Secondary base-station (or cognitive base-station) is a component with cognitive capabilities. Cognitive base-station enables the secondary user access other networks.

There are three different access types in a cognitive network:

- *Secondary network access*: Secondary users can access their own cognitive base station on both licensed and unlicensed bands.

- *Secondary ad hoc access*: Secondary users can communicate with each other through ad hoc connection on both licensed and unlicensed bands.

- *Primary network access*: Secondary users can access the primary base station though the licensed band.

9

2.1.5   Spectrum Sensing

As mentioned above, a cognitive radio system is designed to be aware and adaptable to its surrounding environment. The spectrum sensing ability is used by the cognitive radio to detect spectrum holes. The most direct way to perform that action is to detect the primary users that are receiving data in the communication range of a secondary user. However, it is difficult for a cognitive radio to have a direct measurement of a channel between a primary receiver and a transmitter. For that reason, various techniques have been implemented and focus on primary transmitter detection based on local observations of secondary users. These techniques can be classified as *transmitter detection, cooperative detection*, and *interference-based detection* [5]:

Transmitter detection

Transmitter detection method is based on the detection of the weak signal from a primary transmitter through the local observations of secondary users. If $x(t)$ is the signal received by a secondary user, $s(t)$ is the signal transmitted by the primary user, $n(t)$ is the AWGN and h is the amplitude gain of the channel, then the decision model for the transmitter detection technique can be defined as follows:

$$x(t) = \begin{cases} n(t) & \text{no primary user signal,} \\ hs(t) + n(t) & \text{a primary user signal exists.} \end{cases} \qquad (2.1)$$

There are three schemes used for transmitter detection according to the decision model [16]:

- *Matched filter detection*: When the information of the primary user signal is known to the secondary user, the optimal detector in stationary Gaussian noise is the matched filter since it maximizes the received signal-to-noise ratio (SNR) [5],[16].

- *Energy detection*: If the receiver cannot gather sufficient information about the primary user signal the optimal detector is an energy detector [16].

- *Cyclostationary feature detection*: a cyclostationary feature detector can perform better than the energy detector in noise discrimination because of its robustness to the uncertainty in noise power [5].

Cooperative detection

Cooperative detection exploits the sensing information from other users to make a more accurate decision. With the transmitter detection, the cognitive radio depends on weak primary transmitter signals based on local observations of one secondary user. However, a secondary network is physically separated by the primary network, so that there is no interaction between them. Thus, the secondary user cannot avoid the interference due to the lack of the primary receiver's information [5]. Cooperative detection among unlicensed

users is theoretically more accurate since the uncertainty in a single user's detection can be minimized [17].

Interference-based detection

A new model for measuring interference has been introduced recently by the FCC, the *interference temperature* model. The interference temperature model manages interference at the receiver through the interference temperature limit, which is represented by the amount of new interference that the receiver could tolerate [5]. If the secondary users do not exceed this limit with their transmitting operations, they are allowed to utilize this spectrum band.

2.1.6   Spectrum Analysis

Spectrum analysis enables the characterization of different spectrum bands, which can be used to provide the secondary user with the appropriate band. Since the available spectrum holes show different characteristics over time, depending on the primary user activity and spectrum band informations, it is essential to define some parameters. Those parameters describe the quality of a spectrum band, as follows [5]:

- *Interference*: Depending on the amount of interference at the primary receiver, the permitted power for a secondary user is derived, which is used for the estimation of the channel capacity.

- *Path loss*: As the operating frequency increases, the path loss increases. If the transmission power of a secondary user does not change, then its transmission range decreases at higher frequencies. Accordingly, if transmission power is increased to compensate for the increased path loss, higher interference for other users is caused.

- *Wireless link errors*: The channel's error rate depends on the modulation scheme and the interference level of the spectrum band.

- *Link layer delay*: To address different path loss, wireless link error, and interference, different types of link layer protocols are required at different spectrum bands. This results in different link layer packet transmission delay.

- *Holding time*: The activities of primary users affects the channel quality in cognitive networks. This parameter refers to the expected time duration that the secondary user can utilize a licensed band before getting interrupted.

The parameters described above, define the capacity of the channel, which is the most important feature for spectrum characterization and analysis.

2.1.7   Spectrum decision

Once all available spectrum bands are characterized, the appropriate operating spectrum band can be defined, for the specified Quality of Service (QoS) requirements and the spectrum characteristics. The data rate, acceptable error rate, delay bound, the transmission mode and the bandwidth of the transmission can be determined, based on the user requirements. Consequently, the appropriate spectrum bands can be selected.

2.2   Multiple-Input-Multiple-Output (MIMO) Antenna Systems

In this section, some fundamental knowledge about *Multiple-Input-Multiple-Output Antenna systems* will be presented, concerning their basic technology features and the general MIMO model description, along with some special cases. In section 2.2.2 the utilization of multiple-antennas in a cognitive radio system and its effects are described.

2.2.1   MIMO System description

A Multiple-Input-Multiple-Output (MIMO) system is an antenna system which employs multiple antennas at the transmitter and the receiver, in order to provide space diversity. MIMO technology constitutes a breakthrough in the design of wireless communication systems. MIMO techniques provide significant performance enhancements in terms of quality, data transmission rate and interference reduction. Multi-antennas can be utilized to achieve many desirable enhancements for wireless transmissions, such as folded capacity increase without bandwidth expansion, dramatic increase in transmission reliability via space-time coding and effective co-channel interference suppression for multi-user transmissions [18]. A general block diagram of a MIMO system is depicted in Fig. 2.4.
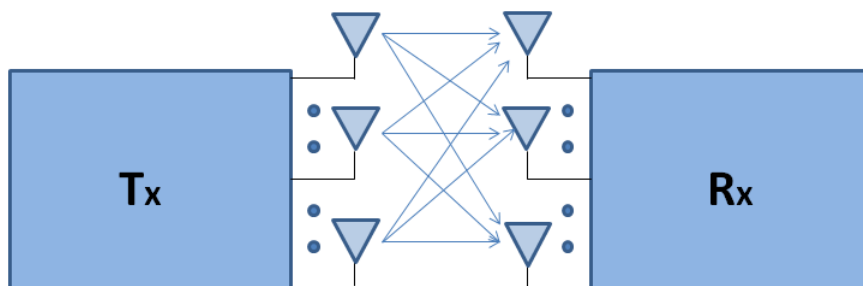
Figure 2.4: General block diagram of a MIMO system

Multiple-input single-output (MISO) systems are special cases of MIMO systems. They employ multiple antennas at the transmitter but only one single antenna at the receiver. Similarly, single-input multiple-output (SIMO) systems have a single antenna at the transmitter and multiple antennas at the receiver.

2.2.2 Cognitive MIMO Systems

The employment of the MIMO technology in cognitive radio systems brings the space diversity to cognitive radio networks. *MIMO cognitive radio systems* employing *beamforming* techniques present a means of improving the throughput of secondary users while minimizing the interference to primary users. Nonetheless, multi-antennas can be used to allocate transmit dimensions in space and hence provide the secondary transmitter with more degrees of freedom in space, in addition to time and frequency, so as to balance between maximizing its own transmit rate and minimizing the interference powers at the primary receivers [18].

However, the merits of MIMO technology in transmission and cognitive radio, in terms of reducing interference and improving secondary link quality, come at the cost of hardware and computational complexity increase. Additionally, complete *Channel State Information (CSI)* at the transmitter is required. CSI refers to the known channel properties of a communication link, representing the effects of *scattering, fading, power decay with distance* and other transmission processes. CSI enables the adaptation of transmissions to current channel conditions, which is crucial for achieving reliable communication with high data rates in multi-antenna systems. Even though CSI at the transmitter is required, research studies on antenna selection in cognitive radio have proved that many of the benefits of MIMO systems can be exploited even if full CSI at the transmitter is not available [3],[8]. As a result, antenna selection is an effective way to exploit spatial diversity in cognitive systems, at reduced cost.

2.3 Orthogonal Frequency Division Multiplexing (OFDM)

Orthogonal frequency-division multiplexing (OFDM) is a method of encoding digital data on multiple carrier frequencies. A large number of closely spaced orthogonal sub-carrier signals are used to carry data on several parallel data streams or channels. Each sub-carrier is modulated with a modulation scheme, such as *QAM (Quadrature Amplitude Modulation)* or *PSK (Phase-Shift Keying)* at a symbol rate, maintaining total data rates similar to conventional single-carrier modulation schemes in the same bandwidth.

2.3.1 OFDM basic characteristics

A significant advantage of Orthogonal Frequency-division Multiplexing over single carrier schemes is its ability to encounter severe channel conditions, without any complex time-domain equalization. Apart from that, OFDM enables the elimination of the *Intersymbol Interference (ISI)*. Intersymbol Interference is defined as the signal's distortion caused by the interference of a symbol with subsequent symbols and is considered as a major factor of communications' degradation. ISI is the result of multipath propagation or the non-linear frequency response of a channel, causing successive symbols to "blur" together [19]. OFDM can cope not only with this form of distortion successfully, but also with

narrow-band co-channel interference.
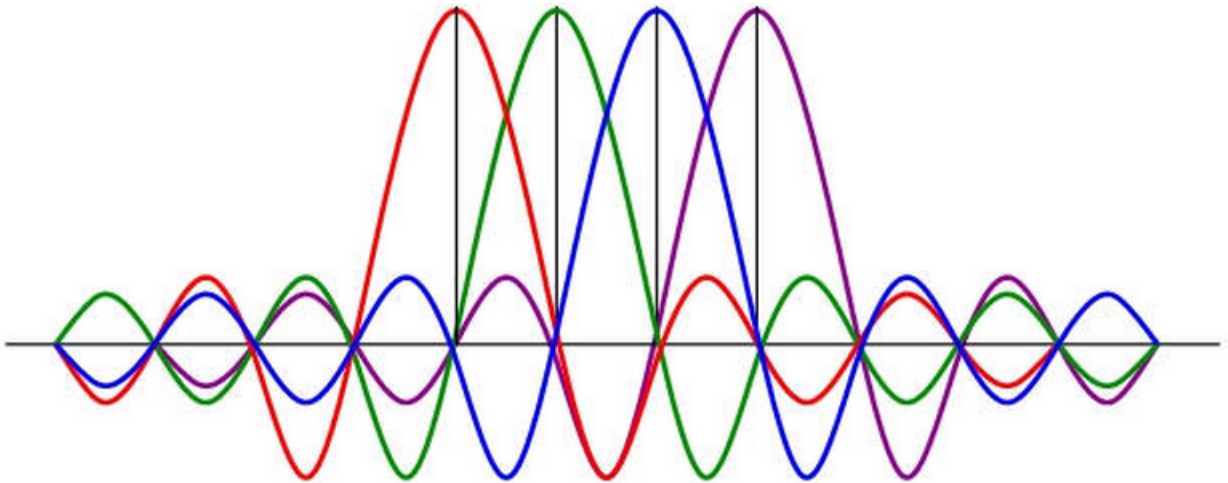
Figure 2.5: Example of the OFDM Spectra

In Fig. 2.5 an example of OFDM spectra is depicted. Four subcarriers can be easily discerned, each one with a different colour. Each subcarrier overlaps in some part all the others. Despite this fact, the receiver can extract the data sent on every subcarrier, due to the scheme's orthogonality: at the maximum energy of each subcarrier (vertical lines), the other subcarriers' energy is zero valued.

If we denote with W the channel bandwidth and Δf is the bandwidth of each subchannel, which is considered narrow enough to consider the characteristics of each subchannel's frequency response ideal, then the number of subcarriers is $N = \dfrac{W}{\Delta f}$. Different data symbols can be transmitted simultaneously through the N subcarriers. For each subchannel, a carrier is utilized, defined as

$$x_k(t) = \sin(2\pi f_k t), \quad k = 0, 1, 2, ..., N - 1 \tag{2.2}$$

where f_k is the central frequency of the k-th subchannel. Orthogonality demands the symbol rate of each subchannel $1/T$ (T denoting the sampling duration) to be equal to Δf, regardless of their relative phase. That leads to

$$\int_0^T \sin(2\pi f_k t + \phi_k) \sin(2\pi f_j t + \phi_j) dt = 0 \tag{2.3}$$

where $f_k - f_j = n/T$, $n = 1, 2, ...$, regardless of the values of the phases ϕ_k and ϕ_j.

The symbol rate in an OFDM system is reduced to a factor of N related to the rate symbol of a single-carrier system which utilizes a bandwidth of W and transmits data in the same rate as the multi-carrier system. Consequently, the symbol duration of an OFDM system is $T = NT_s$, where T_s is the sampling duration of the single-carrier system. By choosing N sufficiently large, ISI can be drastically eliminated.

Since the time synchronization between the subcarriers is retained, OFDM enables the transmission of different number of bits per symbol on each subcarrier. As a result, the subcarriers with higher *Signal-to-Noise Ratio (SNR)* can support more bits per symbol. This important feature enables OFDM to use different modulation schemes to each subcarrier, i.e. a subcarrier can use BPSK, while others use QAM with different constellations.

As previously mentioned, an OFDM system has the ability to completely remove ISI between two OFDM symbols. This is implemented by simply inserting a guard interval between the OFDM symbols, during which all the multipath reflections of the transmitted OFDM symbol fade out, before the next OFDM symbol is transmitted. This guard interval is called *Cyclic Prefix (CP)*. As it is depicted in Fig. 2.6, the Cyclic Prefix is a periodic extension of the last part of an OFDM symbol that is added to the front of symbol in a transmitter, and is removed at the receiver before demodulation.
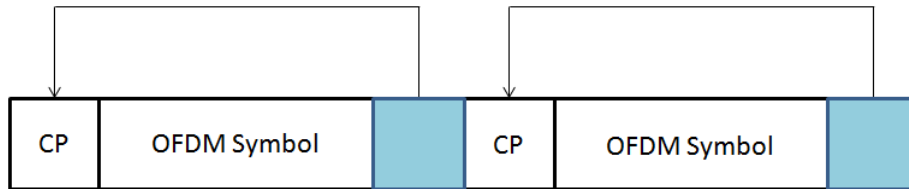
Figure 2.6: Cyclic Prefix

2.3.2 OFDM mathematical description

For a baseband OFDM system model with N subcarriers, each subcarrier can be expressed as:

$$s(t) = e^{j2\pi f_k t}, \tag{2.4}$$

with f_k denoting the carrier frequency of the k-th subcarrier, $f_k = k/NT_s$, where T_s is the symbol duration. Then, the multi-carrier output is given by

$$x(t) = \sum_{k=0}^{N-1} X_k e^{j2\pi k t/NT_s}, \tag{2.5}$$

where X_k is a complex number in a given constellation, such as QPSK or QAM. By considering $t = nT_s$ the OFDM symbol is given by

$$x_n = x(nT_s) = \sum_{k=0}^{N-1} X_k e^{j2\pi nk/N}. \tag{2.6}$$

It should be noted that the above equation is also the equation of an *N-point Inverse Discrete Fourier Transform (IDFT)*, with the exception of the multiplying constant $1/N$. This implies that the demodulation of the signal x_n can be done using a *Discrete Fourier*

Transform (DFT). Usually, a *Fast Fourier Transform (FFT)* is used for the signal demodulation because of the lower computational speed compared to the DFT. Accordingly, an *Inverse Fast Fourier Transform (IFFT)* is used for the signal modulation.

2.3.3 Per-subcarrier Modulation Schemes

As mentioned in 2.3.1, each OFDM subcarrier can be modulated with a different modulation scheme. There are two modulation schemes that are usually employed, *QAM (Quadrature Amplitude Modulation)* and *PSK (Phase-Shift Keying)*.

Quadrature Amplitude Modulation (QAM)

Quadrature Amplitude Modulation is the modulation scheme that constructs signals by impressing separate information bits on each of the quadrature carriers, $\cos(2\pi f_c t)$ and $\sin(2\pi f_c t)$. The transmitted signal waveforms have the form:

$$u_m(t) = A_{mc} g_T(t) \cos(2\pi f_c t) + A_{ms} g_T(t) \sin(2\pi f_c t), \quad m = 1, 2, ..., M \qquad (2.7)$$

where A_{mc} and A_{ms} are the sets of amplitude levels that are obtained by mapping k-bit sequences into signal amplitudes. QAM may be viewed as a form of combined digital amplitude and digital-phase modulation [20]. As in many digital modulation schemes, the constellation diagram is useful for QAM. In QAM, the constellation points are usually arranged in a square grid with equal vertical and horizontal spacing. Since in digital telecommunications the data are usually binary, the number of points in the grid is usually a power of 2 (2, 4, 8,...). The most common forms are 4-QAM, 16-QAM and 64-QAM. Examples of signal space constellations for QAM are shown in Fig. 2.7.

Phase-Shift Keying (PSK)

Phase-Shift keying (PSK) is a digital modulation scheme that conveys data by changing or modulating the phase of a carrier waveform. The general representation of a set of M carrier-phase modulated signal waveform is

$$u_m(t) = g_T \cos(2\pi f_c t + \frac{2\pi m}{M}), \quad m = 0, 1, ..., M-1, \quad 0 \leq t \leq T, \qquad (2.8)$$

where g_T is a baseband pulse shape, which determines the spectral characteristics of the transmitted signal. In PSK, g_T is a rectangular pulse, defined as

$$g_T = \sqrt{\frac{2E_s}{T}}, \quad 0 \leq t \leq T, \qquad (2.9)$$

where E_s denotes the energy/signal or energy/symbol. The corresponding waveform, after viewing the angle of the cosine function, is now

$$u_m(t) = g_T A_{mc}(t) \cos(2\pi f_c t) - g_T A_{ms}(t) \sin(2\pi f_c t), \qquad (2.10)$$
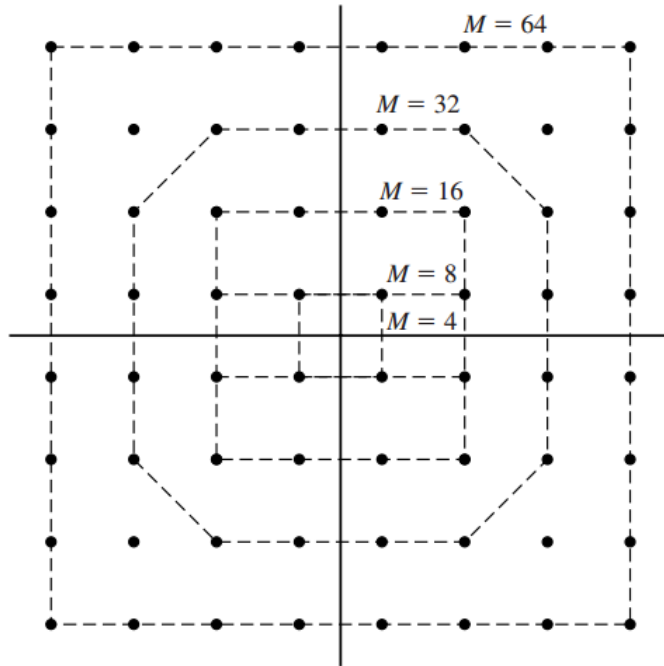
Figure 2.7: Rectangular signal-space constellations for QAM

where $A_{mc} = \cos(2\pi m/M)$ and $A_{ms} = \sin(2\pi m/M)$, it has a constant envelope and the carrier phase changes abruptly at the beginning of each signal interval. Digital phase modulated signals can be represented geometrically as two-dimensional vectors with components

$$s_m = (\sqrt{E_s}\cos(2\pi m/M), \sqrt{E_s}\sin(2\pi m/M)), \qquad (2.11)$$

In Fig. 2.8, significant PSK signal constellations are depicted. If $M = 2$, the modulation scheme is called binary phase-shift keying (BPSK) and its signal constellation is illustrated in Fig. 2.8(a) [20].
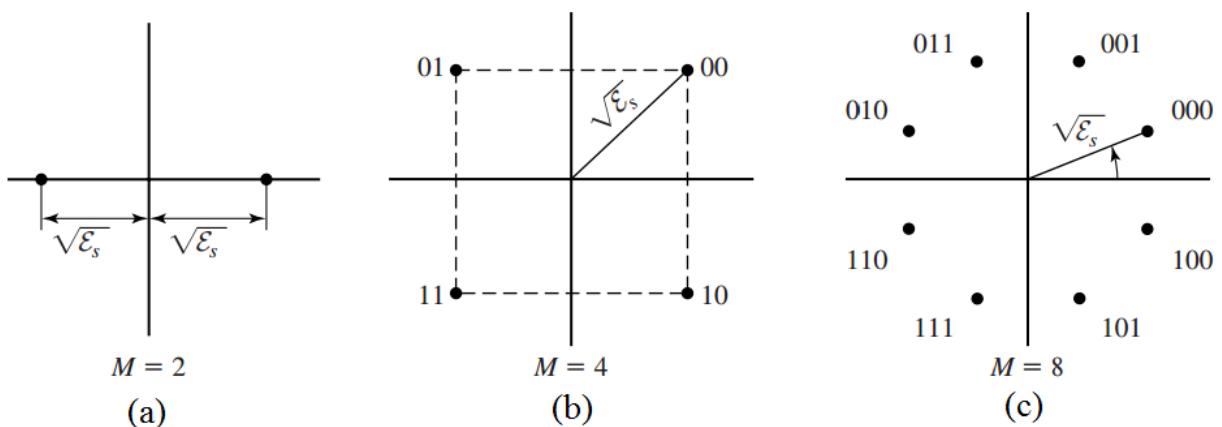
Figure 2.8: PSK signal constellations

2.3.4 Orthogonal Frequency Division Multiple Access (OFDMA)

Orthogonal Frequency Division Multiple Access (OFDMA) is a multi-user version of OFDM. Multiple access is achieved by assigning subsets of subcarriers to multiple users, allowing simultaneous low data rate transmission from several users. Each user in an OFDMA system is usually given certain subcarriers during a certain time to utilize.

One of the most important advantages of OFDMA is that, due to its subcarrier structure, it can support a wide range of bandwidth. A significant advantage stemming from this property, is the *flexibility of deployment*. OFDMA systems can be deployed in various frequency band intervals to efficiently and flexibly correspond to different model system requirements. Other systems, such as *Time Division Multiple Access (TDMA)* and *Code Division Multiple Access (CDMA)*, do not provide such a flexibility in such a natural manner [4]. Since OFDMA is a multiple access scheme version of OFDM, it inherits all the advantages described above.

2.3.5 OFDMA and Cognitive MIMO Systems

OFDMA transmission technologies can be further enhanced with MIMO antenna techniques. As previously mentioned, OFDMA has the ability to eliminate ISI and combat multipath interference. MIMO systems present superb benefits in transmission and cognitive radio, in terms of reducing interference and improving link quality. Moreover, due to the fact that the processing of OFDMA signals provides frequency-flat channels effectively, full MIMO technologies can be combined with OFDMA. OFDM modulation techniques have been actively researched and adopted in various state-of-the-art wireless systems, such as IEEE 802.11 wireless local area network, IEEE 802.16 (WiMAX) and the Third Generation Partnership Project Long-Term Evolution standard, suggesting that OFDM can be adopted as a powerful and flexible modulation scheme for both primary and cognitive radio systems.

2.4 Scalable Video Coding extension of H.264/AVC Standard

Scalable Video Coding (SVC) is a highly attractive solution to the problems posed by the characteristics of modern video transmission systems. The term *scalability* refers to the removal of parts of the video bitstream in order to adapt it to the various needs or preferences of end users, as well as to varying terminal capabilities or network conditions. The resulting substream forms another valid bitstream for some target decoder and the substream represents the source content with a reconstruction quality lower than that of the complete original bitstream, but higher than the quality of the remaining data. The term SVC is used interchangeably for both the concept of SVC in general and for the particular new design that has been standardized as an extension of the H.264/AVC standard. The objective of the SVC standardization has been to enable the encoding of a high-quality video bitstream that contains one or more subset bitstreams that can them-

selves be decoded with a complexity and reconstruction quality similar to that achieved using the existing H.264/AVC design with the same quantity of data as in the subset bitstream [21].

The sophisticated architecture of the SVC extension of H.264 standard is particularly designed to increase the codec capabilities while offering a flexible encoder solution that supports three different types of scalability: temporal, spatial and SNR quality. Spatial scalability and temporal scalability describe cases in which subsets of the bit stream represent the source content with a reduced picture size (spatial resolution) or frame rate (temporal resolution), respectively. In quality scalability, the same spatio-temporal resolution is retained in the resulting substream as in the complete bitstream, but with a lower quality (fidelity) where quality is usually referred to as Signal-to-Noise Ratio (SNR). In the following subsections the three modalities are briefly described and we focus on quality scalability and specifically on *Medium Grain Scalability (MGS)*, which is the video coding scheme we utilize in our work.

2.4.1 Temporal Scalability

The term "temporal scalability" refers to the ability to represent video content with different frame rates by as many bitstream subsets as needed. The motion compensation dependencies are structured so that complete pictures (i.e. their associated packets) can be dropped from the bitstream. Encoded video streams can be composed by three distinct type of frames: *I (intra)*, *P (predictive)* or *B (Bi-predictive)*. *I frames* exploit the spatial prediction from neighboring regions within the picture, while *P* and *B frames* have interrelation with different pictures, as they exploit directly the dependencies between them. Temporal scalability with dyadic temporal enhancement layers can be provided with the concept of *hierarchical B-pictures*, as depicted in Fig. 2.9. The numbers below the pictures specify the coding order, the symbols T_k specify the temporal layers and k is the corresponding temporal layer. Group of Pictures (GOP) is defined as the group of pictures between two successive pictures of the base layer and the next base layer picture [21].

2.4.2 Spatial Scalability

In spatial scalability, the video stream is coded at multiple spatial resolutions (Fig. 2.10). The data and decoded samples of lower resolutions can be used to predict data or samples of higher resolutions in order to reduce the bit rate to code the higher resolutions. In each spatial layer, motion compensated prediction and intra-prediction are employed as for single-layer coding. In order to improve coding efficiency in comparison to simulcasting different spatial resolutions, additional *Inter-Layer Prediction (ILP)* mechanisms are employed. The main goal of the ILP module is to increase the amount of reused data in the prediction from inferior layers, so that the reduction of redundancies increases the overall efficiency. Three prediction techniques are supported by the ILP module: *Inter-Layer*
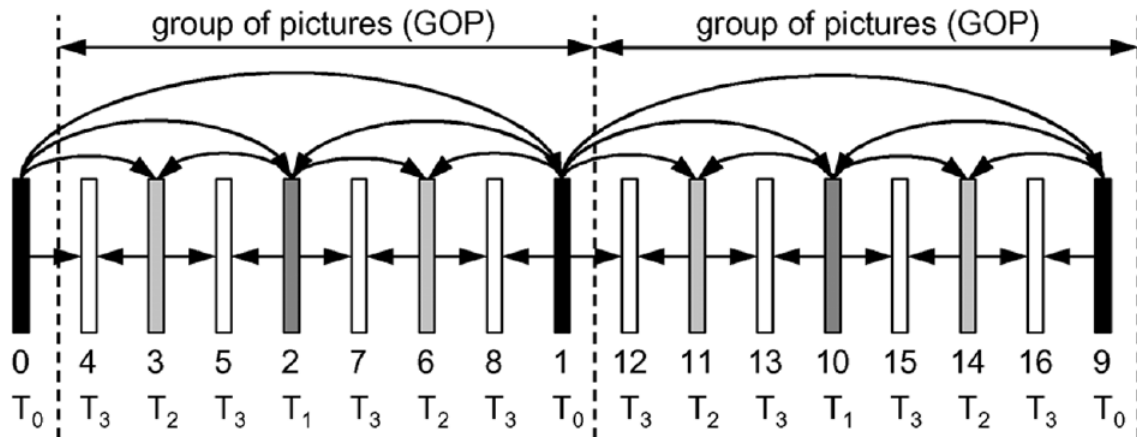
Figure 2.9: Temporal Scalability, Hierarchical B-pictures

Motion Prediction, where the motion vectors from lower layers can be used by superior enhancement layers, *Inter-Layer Intra Texture Prediction*, where texture for internal blocks within the same reference layer (intra) is predicted, and *Inter-Layer Residual Prediction*, which can be used after the motion compensation process to explore redundancies in the spatial residual domain.
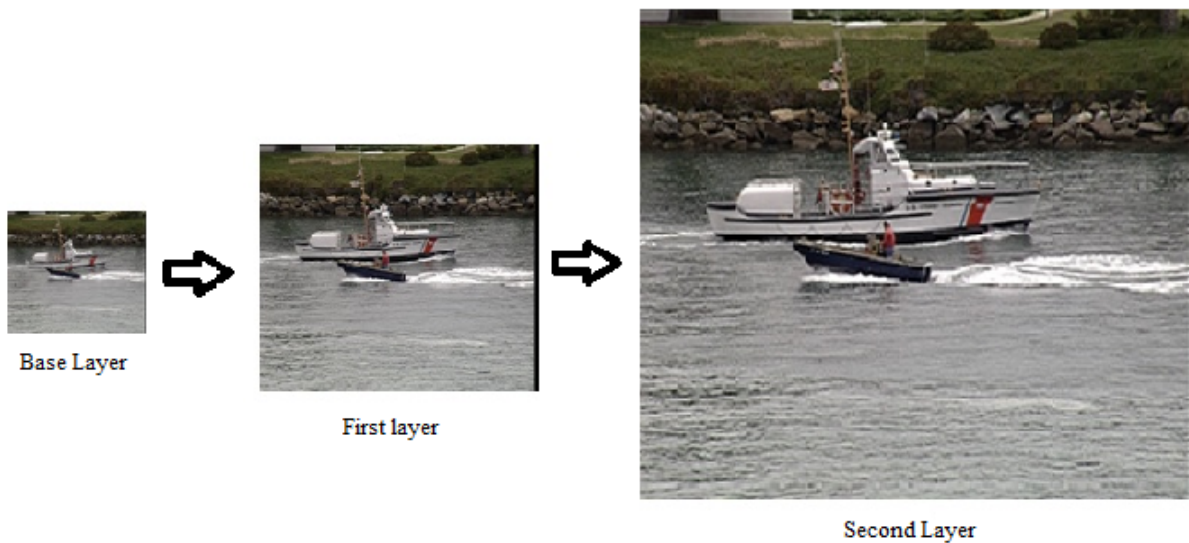
Figure 2.10: Spatial Scalability example, different spatial resolutions

2.4.3 Quality Scalability

In quality (SNR) scalability, the video stream is coded at the same spatio-temporal resolution but at different qualities (Fig. 2.11). Quality scalability can be considered as a special case of spatial scalability with identical picture sizes for base and enhancement

layer [21]. A significant feature of this type of scalability is that the data and decoded samples of lower qualities can be used to predict data or samples of higher qualities in order to reduce the bit rate to code the higher qualities. Quality scalability is based on using distinct *Quantization Parameters (QP)* for each layer. The Quantization Parameter defines the step size for associating the transformed coefficients of the difference between the source and prediction signals, into the spatial frequency domain, with a finite set of steps. Smaller values of QP indicate better video quality, thus higher bit rate, while larger values of QP determine worse video quality and lower bit rate. There are two quality scalability modalities:

- Coarse Grain Scalability (CGS): CGS can support only a predefined set of rate-distortion points [8]. Moreover, each layer has an independent prediction procedure. The same inter-layer prediction mechanisms as for spatial scalable coding are employed, but without using the corresponding up-sampling operations [21]. The CGS strategy can be regarded as a special case of spatial scalability when consecutive layers have the same resolution [22].

- Medium Grain Scalability (MGS): It it the modality employed in our system model. With the MGS scheme the flexibility of bitstream adaptation and error robustness are increased. Moreover, MGS strategy improves the coding efficiency for bit streams that have to provide a variety of bit rates. Efficiency is increased by employing a more flexible prediction module, where different layer types can be referenced. However, this strategy can introduce a synchronism offset between the encoder and the decoder (*drift*), if only the base layer is received. To overcome this issue, periodic *key pictures* are used to immediately resynchronize the prediction loops at encoder and decoder.

Figure 2.11: Quality Scalability example, different number of layers

CHAPTER 3

RESOURCE ALLOCATION METHODOLOGY

3.1 System Model

In this section, the considered system model is described, based on the background knowledge provided in the previous chapter. In section 3.1.1, the radio network is presented and in section 3.1.2 we describe the proposed video coding scheme.

3.1.1 Radio Network

We consider an OFDMA multiple-input-single-output (MISO) cognitive radio system which co-exists with a Primary User Network, as shown in Fig. 3.1. The two networks share the same spectrum. The secondary base station (SU-Tx) is equipped with M antennas and transmits data to K different single antenna secondary users. The same configuration as in [8] and [6] is employed, where it is assumed that the primary transmitter is far enough from cognitive users such that the interference power from the primary transmitter to the secondary receivers is much less than the signal power from the secondary transmitter to the secondary receivers. Consequently, the interference at the secondary receivers can be accumulated in the noise power.

The bandwidth is divided into N subcarriers, which are shared by the two networks. We denote with $\mathbf{H}_k$ the channel gains between the cognitive base station and the kth SU
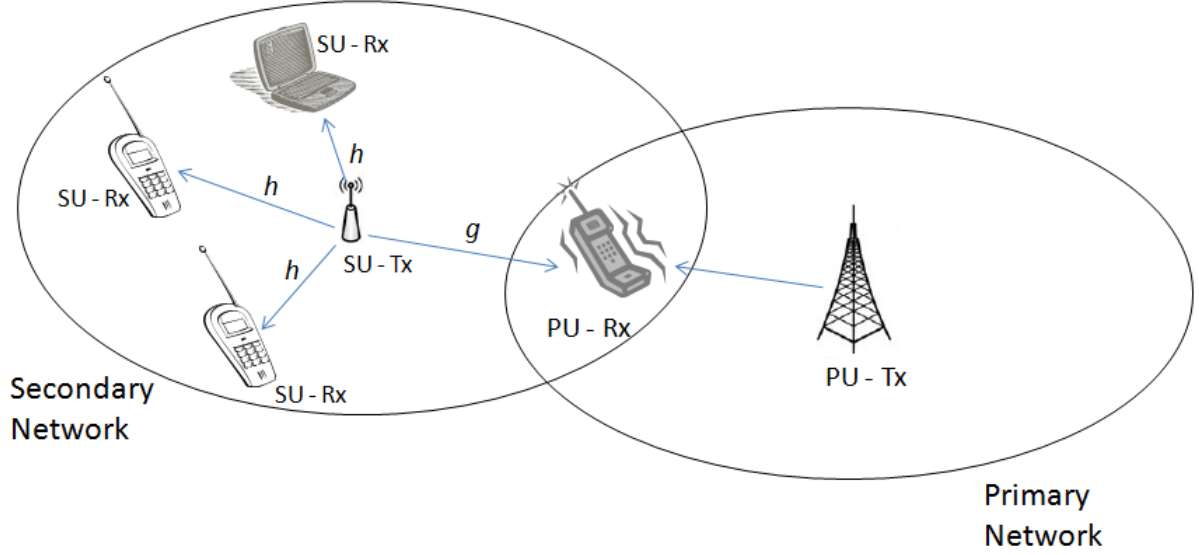
Figure 3.1: System Model

and with $\mathbf{G}$ the interference channel between the cognitive transmitter and the primary receiver. These quantities are defined as,

$$\mathbf{H}_k = \begin{bmatrix} h_{1,1}^k & h_{1,2}^k & \cdots & h_{1,M}^k \\ h_{2,1}^k & h_{2,2}^k & \cdots & h_{2,M}^k \\ \vdots & \vdots & \ddots & \vdots \\ h_{N,1}^k & h_{N,2}^k & \cdots & h_{N,M}^k \end{bmatrix}, \tag{3.1}$$

where $h_{n,m}^k$ is the frequency response of the kth SU from the mth transmit antenna of the cognitive base station through the nth subcarrier and,

$$\mathbf{G} = \begin{bmatrix} g_{1,1} & g_{1,2} & \cdots & g_{1,M} \\ g_{2,1} & g_{2,2} & \cdots & g_{2,M} \\ \vdots & \vdots & \ddots & \vdots \\ g_{N,1} & g_{N,2} & \cdots & g_{N,M} \end{bmatrix}, \tag{3.2}$$

where $g_{n,m}$ is the channel power gain between the primary receiver and the mth transmit antenna of the cognitive base station through the nth subcarrier. It is assumed that the cognitive system has perfect knowledge of the channels between the secondary transmitter and the primary receiver and that between the secondary transmitter and the secondary receivers.

Considering the OFDM modulation with overlapping subcarriers that both primary and secondary system use and in order to ensure the protection of the primary network communications, an interference power limit is imposed on a per-subcarrier basis, as in [8]. If we imposed a sum interference power limit on this system, a number of subcarriers might experience very high interference power, leading to unacceptable data loss for the licensed user. If $I_{\max}$ is the interference power limit we described, then the maximum power that

can be loaded on the nth subcarrier by the mth antenna of the cognitive transmitter is given by

$$\bar{p}_{n,m} = \min \left(\frac{I_{\max}}{|g_{n,m}|^2}, p_{\max} \right), \quad (3.3)$$

where $p_{\max}$ is the maximum power that the transmitter can load on any subcarrier. In this framework, a single primary user is considered. However, all the presented techniques can be extended to multiple primary users that access the channel. In this case, the maximum power that can be loaded on each subcarrier at the cognitive transmitter would depend on the channel gains of the primary users to which the subcarriers are assigned.

We consider a system that employs M-ary quadrature amplitude modulation (M-QAM) and binary phase-shift keying modulation (BPSK) as modulation schemes per subcarrier, with $M = \{4, 16, 64\}$. By this formulation, BPSK is used to carry one bit/symbol, while 4-QAM, 16-QAM and 64-QAM are used to carry two, four and six bits/symbol respectively.

The maximum number of bits that can be loaded on each subcarrier can be computed given a target bit error rate (BER). For M-QAM, the bit-error probability is upper bounded by the symbol error probability, which is tightly approximated by $4Q[\sqrt{d^2/(2N_o)}]$, where d is the minimum distance between the points in the signal constellation. Since the average energy of a M-QAM symbol is equal to $(M-1)d^2/6$, the required power for carrying c bits/symbol at a given BER is

$$E = \frac{N_o}{3} \left[Q^{-1} \left(\frac{P_e}{4} \right) \right]^2 (2^c - 1). \quad (3.4)$$

Consequently, the SNR required to achieve a target BER, P_e, for 2^c-ary QAM, is calculated using

$$\gamma = \frac{1}{3} \left[Q^{-1} \left(\frac{P_e}{4} \right) \right]^2 (2^c - 1) \quad (3.5)$$

and for BPSK modulation using

$$\gamma = \frac{1}{2} \left[Q^{-1} \left(P_e \right)^2 \right], \quad (3.6)$$

where Q is the Q-function, which gives the probability that a single sample taken from a random process with zero-mean and unit-variance Gaussian probability density function will be greater or equal to x:

$$Q(x) = \frac{1}{\sqrt{2\pi}} \int_x^\infty e^{-t^2/2} dt = \frac{1}{2} erfc \left(\frac{x}{\sqrt{2}} \right), \quad x \geq 0 \quad (3.7)$$

It has been proved ([8]) that the difference of the PSNR (Peak Signal-to-Noise Ratio) of a reception compared to the PSNR of an error-free reception is minimal when BER has a value of 10^{-6}. To have a BER $P_e = 10^{-6}$, the calculated SNR values for different modulation schemes are depicted in Table 3.1. The fourth column presents the number

Table 3.1: Required SNR to attain $P_e = 10^{-6}$ for different modulation schemes and the corresponding number of bits/symbol.

Case	Modulation	$\gamma_{case}(dB)$	Bits per symbol
1	BPSK	10.53	1
2	4-QAM	14.03	2
3	16-QAM	21.01	4
4	64-QAM	27.25	6

of bits per symbol that each modulation scheme supports. To find the maximum number of bits that can be loaded on the nth subcarrier of kth SU by the mth antenna $c_{k,n,m}$, we compute,

$$\gamma_{k,n,m} = \bar{p}_{n,m} \frac{|h_{n,m}^k|^2}{\sigma_v^2},$$

(3.8)

where σ_v^2 is the noise variance, which is assumed to have the same value for all the subcarriers. It should be mentioned here that if the interference from the primary transmitter to the secondary receivers were not considered negligible, the term σ_v^2 must be replaced by $\sigma_v^2 + \sigma_i^2$, where σ_i^2 is the interference power from the primary transmitter. The modulation scheme, thus the maximum number of bits supported by the subcarrier, is then determined by the following:

$$
\begin{array}{llll}
\text{if} & \gamma_1 \leq \gamma_{k,n,m} \leq \gamma_2 & \text{then} & c_{k,n,m} = c_1 = 1, \\
\text{if} & \gamma_2 \leq \gamma_{k,n,m} \leq \gamma_3 & \text{then} & c_{k,n,m} = c_2 = 2, \\
\text{if} & \gamma_3 \leq \gamma_{k,n,m} \leq \gamma_4 & \text{then} & c_{k,n,m} = c_3 = 4, \\
\text{if} & \gamma_{k,n,m} \geq \gamma_4 & \text{then} & c_{k,n,m} = c_4 = 6.
\end{array}
$$

3.1.2 Video coding scheme (H.264 SVC Extension - MGS)

As mentioned in section 2.4, the Scalable Video Coding extension of the H.264 standard has been chosen for the sequences' coding, because it provides QoS enhancement for each user and adapts to the CR systems fluctuations by selectively discarding video packets. Each cognitive secondary user receives an encoded video sequence. The SVC quality scalability mode enables the generation of substreams having different quality levels (layers). Depending on the bit loading method that we described, each user receives data at a specific bit rate, which determines the substreams that will be transmitted. In Fig. 3.2 we demonstrate a graph that shows the relationship between the Peak-Signal-to-Noise Ratio (PSNR) and bit-rate for a MGS encoded sequence. The extractable rate points and the corresponding PSNR values were obtained by JSVM (Joint Scalable Video Model) software V. 9.19.14, Fraunhofer HHI.

PSNR suggests a quality measure and we can identify 13 levels of quality (layers) for different rate values. An important observation is that an increase in rate does not lead to an increase in quality between extractable points, but results in utilizing unnecessary resources for the same outcome. This is taken into consideration in the problem's formulation.
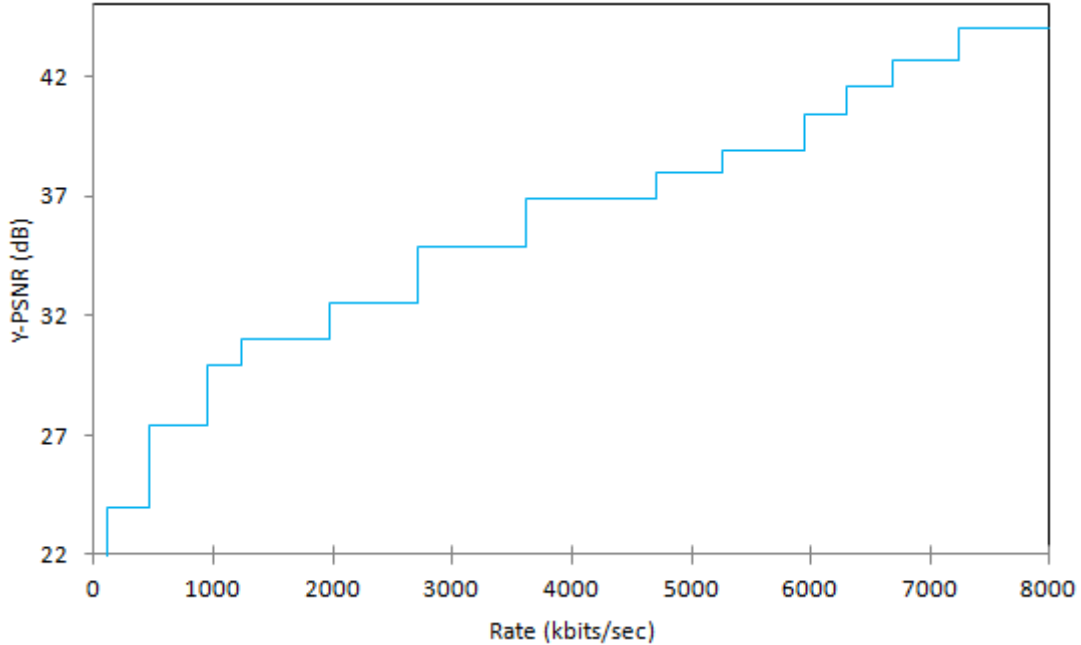
Figure 3.2: Quality-rate plot with MGS encoding for "Bus" sequence.

3.2 Nash Bargaining Solution Resource Allocation Method (NBSm)

This resource allocation method is based on a Game Theory framework, performing a bargaining game where the secondary users of the cognitive radio systems are considered as the players. The bargaining game is one kind of cooperative games where the players, who have conflicts of interest, have the opportunity to reach a mutually beneficial agreement. A Bargaining Solution produces the pay-off where all the users agree on, not just for one bargaining problem but for all bargaining problems. We are especially interested in the Nash Bargaining Solution (NBS).

3.2.1 Nash Bargaining Solution

In the Nash bargaining game, two or more players demand a portion of a utility. If the total amount requested by the players is less than that available, both players get their request. On the other hand, if their request is greater than that available, neither player gets their request. A Nash bargaining solution is a *Pareto efficient* solution to a Nash

bargaining game. This means that this kind of solution is produced after reaching a state where it is impossible to improve any player's gain without reducing another's.

A K-player bargaining problem is a pair $\langle X, (d_1^0, d_2^0, ..., d_K^0) \rangle$, where X is a compact and convex set, and there exists at least one utility set $(x_1, x_2, ..., x_K) \in X$, for which $x_k > d_k^0, \quad k = 1, 2, ..., K$. A bargaining solution is a function F that assigns a bargaining problem $\langle X, (d_1^0, d_2^0, ..., d_K^0) \rangle$ to a unique element of X. The vector $d = (d_1^0, d_2^0, ..., d_K^0)^T$ consists of the *disagreement points*, which express the value of the utility each player can expect to receive, when negotiations break down. The *Nash Bargaining Solution (NBS)*, is the solution set that maximizes the *Nash product*:

$$(\tilde{x_1}, \tilde{x_2}, .., \tilde{x_K}) = \arg\max(x_1 - d_1^0)^{bp_1}(x_2 - d_2^0)^{bp_2} \cdots (x_K - d_K^0)^{bp_K}, \qquad (3.9)$$

subject to $x_k > d_k^0$, $\forall k$ and $\sum_{k=1}^{K} bp_k = 1$. The value bp_k is the *bargaining power*, which is a weighting factor that expresses the advantage of a player over the others, in the bargaining procedure. When a player has a higher bargaining power, the bargaining game favours him over the others and when all players have the same value of bargaining powers, then they are all considered equal to each other.

A pay-off pair x is feasible if the players can agree on a deal that results in their receiving the pay-offs specified by x. We always assume that the set X of feasible pay-off pairs satisfies three requirements:

- The set X is convex.

- The set X is closed and bounded above, which means that the set contains all its boundary points and there exists b, so that $x \leq b$, $\forall x$ in the set.

- *Free disposal* is allowed.

Free disposal is the player's ability to dispose of utility and it is usually a harmless addition. If x is a pay-off profile on which the players can agree and $x \geq y$, then the players can achieve y by agreeing that each player will dispose of a certain amount of utility, after x has been implemented. Fig. 3.3 illustrates the difference in the co-operative pay-off region, when free disposal is permitted.

John Nash introduced four axioms that any generalized Nash Bargaining Solution must satisfy [28]:

1. The bargaining solution lies in the bargaining set.

   (a) $F(X, d) \geq d$,

   (b) $y \geq F(X, d) \Rightarrow y \notin X$.

2. The final outcome does not depend on how the players calibrate their utility scales. This means that, given any strictly increasing affine transformation τ, then

$$F(\tau(X), \tau(d)) = \tau(F(X, d)).$$

27
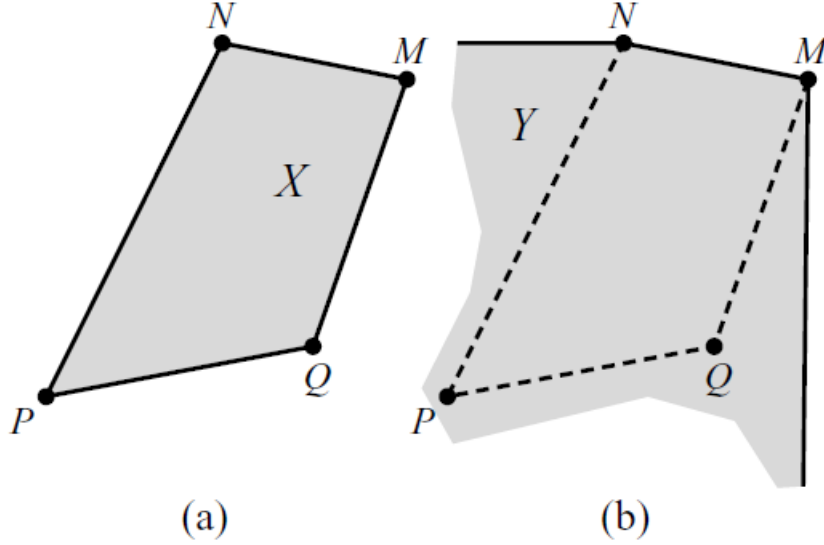
Figure 3.3: Co-operative pay-off regions (a)without permitting free disposal and (b)permitting free disposal

3. If the players sometimes agree on the pay-off pair s when t is feasible, then they never agree on t when s is feasible *(Independence of Irrelevant Alternatives)*. In Fig. 3.4 the set Y is a subset of X that contains $F(X,d)$. The elements of X that are not in Y are irrelevant alternatives. If the bargaining solution selects $F(X,d)$ for the bargaining problem (X,d), then it should also select $F(X,d)$ for the bargaining problem (Y,d) because the choice should be independent of the availability or unavailability of irrelevant alternatives: if $d \in Y \subseteq X$, then

$$F(X,d) \in Y \Rightarrow F(Y,d) = F(X,d).$$

4. In symmetric situations, both players get the same amount of utility. This axiom declares that the bargaining solution does not depend on who is player with label A and who is player with label B. If the labels are reversed, each will still get the same pay-off. If function ρ is defined by $\rho(x_1, x_2) = (x_2, x_1)$, then

$$F(\rho(X), \rho(d)) = \rho(F(X,d)).$$

3.2.2 Problem formulation

This method focuses on allocating resources is such a way that provides mutual agreement of the users (fairness). Based on Nash Bargaining Solution theory described in 3.2.1, one of our major concern is the maximization of Nash product. For our problem, the K players of the Bargaining Game are the K secondary cognitive users and the utilities for which they bargain, are the Peak Signal-to-Noise Ratio (PSNR) values $d_1, d_2, ..., d_K$. The NBS of (3.9), which maximizes the Nash product, now becomes
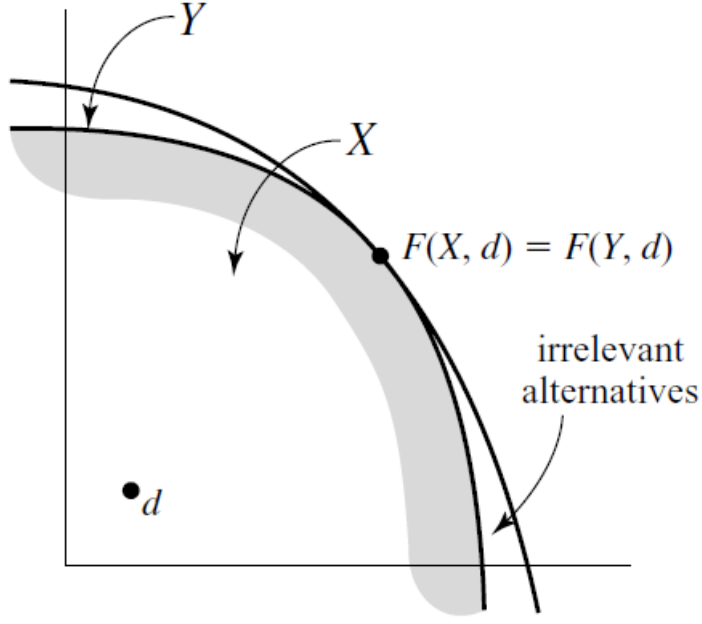
Figure 3.4: Irrelevant Alternatives

$$(\tilde{d}_1, \tilde{d}_2, .., \tilde{d}_k) = \arg\max \prod_{k=1}^{K} (d_k - d_k^0)^{bp_k}, \text{ with } d_k > d_k^0, \ \forall k, \tag{3.10}$$

where d_k is the received PSNR for user k, and $d^0 = (d_1^0, d_2^0, ..., d_K^0)^T$ is the vector of the *disagreement points*.

As mentioned in 3.1, the secondary base station (SU-Tx) is equipped with M antennas and transmits data to K different single antenna secondary users. The bandwidth is divided in N subcarriers. The problem formulation continues with the introduction of an indicator variable $\alpha_{k,n,m}$, which is defined as:

$$\alpha_{k,n,m} = \begin{cases} 1, & \text{if user } k \text{ receives from the } m\text{th} \\ & \text{antenna through the } n\text{th subcarrier}, \\ 0, & \text{otherwise.} \end{cases} \tag{3.11}$$

The rate at which kth user receives through all the antennas and subcarriers assigned to him, can be expressed as,

$$r_k = \sum_{m=1}^{M} \sum_{n=1}^{N} c_{k,n,m} a_{k,n,m}. \tag{3.12}$$

If r_k is determined, the visual quality of the sequence of kth user, $d_k(r_k)$, can be defined by using the quality-rate plot, as the one presented in Fig. 3.2.

Apart from the maximization of the Nash product, another major concern is the minimization of resources' waste. As mentioned above, given the staircase quality-rate

form of the MGS sequence, a higher bit-rate does not always lead to PSNR improvement. For instance, in Fig. 3.2 at a rate of 3000 kbits/sec a user receives PSNR = 36.88 dB and, at a rate of 3500 kbits/sec, receives the same quality leading to a waste in resources. Moreover, due to the fact that many possible solutions were produced by considering only the maximization of the Nash product, a restriction should be imposed to limit those results. With respect to this, we introduce a penalty term that expresses the difference between the rate at which each user receives the substream and the actual rate for achieving the same quality level. The resource allocation solution can now be formulated as,

$$\alpha = \arg\max \left[W_1 \prod_{k=1}^{K}(d_k - d_k^0)^{bp_k} - \sum_{k=1}^{K}(r_k - r_{k,l}) \right], \quad (3.13)$$

under the constraint,

$$\sum_{k=1}^{K}\sum_{m=1}^{M} \alpha_{k,n,m} = 1, \ \forall n, \quad (3.14)$$

where α is the allocation matrix consisting of the elements $\alpha_{k,n,m}$; d_k^0 is the element of the disagreement point vector of the Nash bargaining solution that corresponds to k-th user, which we consider to be the PSNR of the base layer of the video sequence transmitted to each secondary user, to ensure that each user will receive the minimum QoS; and $r_{k,l}$ is the minimum rate to achieve the distortion level that the kth user achieves. The first term of the objective function concerns the maximization of Nash product and the second part is the penalty term mentioned above. The constant W_1 is a weight factor (generally a large number), which implies that the maximization of the Nash product is more important than the minimization of the resources waste [8]. By assigning a large enough number to W_1, the maximization process will always converge to the solution at the higher number of layers. The constraint 3.14 is introduced to state that any subcarrier can be assigned to exactly one secondary user and one antenna. It should be noted that in this problem formulation, the relationship between transmission rate and video quality is known, as there values can be derived from the encoding process described in 3.1.2.

3.3   Aggregate Visual Quality Resource Allocation Method (AVQm)

In this section the resource allocation method for allocating subcarriers and antennas among multiple cognitive users such that the aggregate visual quality of all video sequences is improved while minimizing the unnecessary utilization of resources, is presented. Based on the rate-quality characteristics of the encoded video sequence, provided by the R-D plot (i.e. Fig. 3.2), the PSNR value that corresponds to the rate each user receives the video sequence can be extracted. It follows that a candidate objective function for the

resource allocation problem would be

$$\max_{r_k} \quad d_k(r_k) \tag{3.15}$$

where r_k is the rate achieved by k-th user and d_k is the PSNR value achieved at this rate. However, as already described, because of the staircase quality-rate form of the MGS sequence does not always lead to visual quality enhancement. To encounter this difficulty, we introduce the penalty term described in 3.2.2. The formulation of the objective function focuses on the maximization of the aggregate visual quality as described in [8] and the resource allocation problem solution for this formulation is,

$$\alpha = \arg\max \left[W_2 \sum_{k=1}^{K} d_{k,l} - \sum_{k=1}^{K} (r_k - r_{k,l}) \right], \tag{3.16}$$

under the constaint,

$$\sum_{k=1}^{K} \sum_{m=1}^{M} \alpha_{k,n,m} = 1, \ \forall n, \tag{3.17}$$

where α is the allocation matrix consisting of the elements $\alpha_{k,n,m}$; d_k is the PSNR value obtained if user k receives all layers up to the lth layer, and $r_{k,l}$ is the minimum rate to achieve the distortion level that the kth user achieves. The first part of the objective function corresponds to the maximization of the sum visual quality for all the secondary users, while the second part indicates the difference between the rate at which each user receives the substream and the actual rate for achieving the same quality level. To favour the first part of the objective function (maximization of aggregate visual quality) we introduce W_2, as the corresponding weight factor mentioned above, which has a large value. The constraint of assigning any subcarrier to at most one SU and one antenna (equation 3.17) applies to this objective function as well, in addition to each cognitive user's receiving at least the base layer.

3.4 Particle Swarm Optimization

To solve the formulated problem, the employed optimizer is the *Particle Swarm Optimization* (PSO) algorithm due to its efficiency in similar problems [30], [31] and the fact that it has the ability to deal with discrete values, with low computational complexity. Particle Swarm Optimization is a stochastic optimization algorithm that belongs to the category of *swarm intelligence* methods and draws inspiration from the social dynamics of living organisms.

The optimizer utilizes a *swarm* of search points, called *particles*, which simultaneously and iteratively move in the search space with an adaptable velocity, locating the most promising regions. Each particle has a memory where it retains the best position it has ever visited in the search space, which can be communicated also to (some of) the rest. Each particle assumes a set of other particles to be its *neighbours* and it shares its best

visited position only with them, instead of with the whole swarm. Particles alter their position and velocity according to the other particles that belong to their *neighbourhood.* The particles belonging to a neighbourhood form a *neighbourhood topology,* which is a scheme representing the connections between the particles (nodes) of a neighbourhood [25]. The most common type or neighbourhood topology is the *ring topology,* depicted in Fig. 3.5.
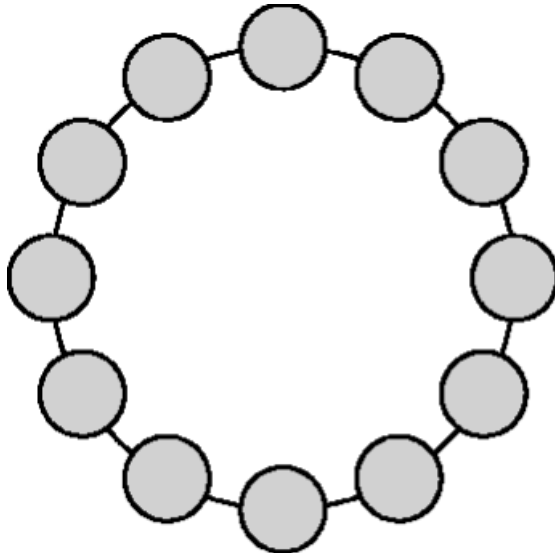
Figure 3.5: Ring topology.

Let the swarm $S\{X_1, X_2, X_3, ..., X_N\}$ consist of N particles. Each particle is a n-dimensional vector $X_i \in \mathcal{S}$, $i = 1, 2, \ldots, N$, where $\mathcal{S}$ is the search space. Let V_i and P_i denote the velocity and the best position, respectively, of the ith particle, and g_i the index of the particle that attained the best previous position among all the particles in the neighbourhood of X_i. If t denotes the current iteration, the velocity and position of X_i are updated according to the following equations:

$$
\begin{aligned}
V_i(t+1) &= \chi \left[V_i(t) + C_1 R_1 \left(P_i(t) - X_i(t) \right) + C_2 R_2 \left(P_{g_i}(t) - X_i(t) \right) \right], \quad (3.18) \\
X_i(t+1) &= X_i(t) + V_i(t+1), \quad (3.19)
\end{aligned}
$$

where χ is the *constriction coefficient*; C_1 and C_2 are positive constants, also known as *cognitive* and *social* parameter, respectively; and R_1 and R_2 are random vectors with components uniformly distributed within the range $[0, 1]$. All vector operations in Eqs. (3.18) and (3.19) are performed componentwise [25]. Assume that a function $f(x)$ is to be minimized. At each iteration, after the update and evaluation of particles, best positions are also updated. The new best position of X_i at iteration $t + 1$ is defined as follows:

$$
P_i(t+1) = \begin{cases} X_i(t+1), & \text{if } f(X_i(t+1)) \leq f(P_i(t)) \\ P_i(t), & \text{otherwise.} \end{cases}
$$

The new determination of index g_i for the updated best positions completes a PSO iteration. The particles are usually initialized randomly.

Clerk and Kennedy [29], after investigating the stability of PSO algorithm, proposed a set of parameter values for χ, C_1 and C_2 that lead to algorithm's convergence to the optimal solutions, namely $\chi = 0.729$, $C_1 = C_2 = 2.05$.

The resource allocation variable $\alpha_{k,n,m}$ indicates the CS transmission antenna and the user each subcarrier is assigned to. If N is the number of subcarriers, K the number of secondary users, and M the number of transmit antennas, then $\alpha_{k,n,m}$ could be represented as a set of $M \times N$ vectors of K elements, where each element k belongs in $\{0,1\}$ and each array can contain at most one element valued 1, because (as mentioned in Section 3.2.2) each subcarrier can be assigned to only one user and one transmit antenna. Additionally, with respect to this restriction, exactly one non-zero single vector and $M - 1$ zero-valued vectors can be assigned to each subcarrier. There are $K + 1$ possible single vectors representations. For illustration purposes, we consider the case where $K = 3, N = 64$ and $M = 2$. The indicator variable $\alpha_{k,n,m}$ can be represented as a set of $2N = 128$ single vectors of three (K) elements and there is a set of four $(K + 1)$ possible single vector representations: $[0, 0, 0], [1, 0, 0], [0, 1, 0], [0, 0, 1]$. This formulation sets the dimension of the problem to $(K + 1)^{M \times N}$.

To perform a dimensionality reduction, we adopted the following formulation: since only one antenna transmits to one user through a subcarrier, we can employ N integers (expressing each subcarrier) to indicate to which antenna the non-zero vector is assigned (expressing which antenna is being used by this subcarrier), and N integers expressing which non-zero vector this is. This leads to a $(2N)$-dimensional vector. In the previous example, a 128-element vector is constructed with the first 64 elements indicating which antennas are being used by the 64 subcarriers, respectively, and the next 64 elements indicating which user is being serviced by this pairing. With this formulation, the dimension is reduced to $(M \times K)^N$.

CHAPTER 4

EXPERIMENTAL RESULTS

In this chapter, the results of the experiments that were conducted to evaluate the proposed methods are presented. For each testing case, a number of experiments was performed, with different channel simulation settings and system configuration. Initially, the system settings and the metrics used for the evaluation of the methods are presented. After introducing these prerequisite descriptions, the results of the experiments are presented.

4.1 System Configuration and Simulation Settings

This section describes and presents the settings of the channel and the video encoding parameters that were used to produce the experimental results.

4.1.1 Channel Settings

The frequency selective fading channel consisted of L=8 Rayleigh fading paths. The channel fading between users and channels were modeled as an independent and identically distributed complex Gaussian. The Rayleigh multipath fading is defined in the time domain by

$$R(t) = \sum_{t=0}^{L-1} \tilde{a}_l \delta(t - lT), \tag{4.1}$$

where $\tilde{a}_l$ is the complex amplitude of path l and L is the number of channel taps: $\tilde{a}_l = \chi_l + j\psi_l$, where χ_l and ψ_l are normally distributed. The frequency domain channel is given by its Fourier Transform.

We considered $M = 4$ antennas at the cognitive base station, contributing to inter-ference reduction to multiple users and rate performance enhancement. The number of the subcarriers N, the number of the cognitive users K and the Channel-to-Noise ratio CNR, were the parameters modified for each simulation case. The CNR is defined as

$$CNR = \frac{\sum_{l=0}^{L-1} E[|\tilde{a}_l|^2]}{N_o}. \tag{4.2}$$

An interference power limit $I_{max} = 0.2$ units of power was imposed on every subcarrier. This threshold ensured that the primary user's data on any subcarrier are not lost due to secondary transmission. The maximum transmit power on any subcarrier was $p_{max} = 1$ unit of power. The rate at which the symbols were transmitted was set to $R_s = 10800$ symbols/sec (54 OFDM symbols in $5msec$ transmission frame period).

4.1.2   Video Encoding Settings

Four video sequences were considered for the experiments: "Bus", "Foreman", "Coast-guard" and "Akiyo" sequences, obtained in 4:2:0 YUV format [32]. The first three se-quences are high-motion while "Akiyo" is a low-motion sequence. For the encoding pro-cess, the JSVM 9.19.14 software was used [23]. The four different video sequences were obtained in *Common Intermediate Format (CIF)* (spatial 352×288 resolution) and were encoded at 30 frames per second using MGS techniques. Each bitstream was encoded in five video layers, one base layer with quantization parameter $QP_b = 48$, and four en-hancement layers with quantization parameters $QP_l = (16, 24, 32, 40)$. To generate the MGS bitstream, each enhancement layer was split further into three MGS enhancement layers and the MGS vectors chosen in the encoding process were $[4, 4, 8]$.

To obtain the rate-quality plots for the SNR scalable bitstreams, a set of 13 rate points were extracted and decoded from each scalable bitstream, representing the 13 quality layers of the video sequence. The results are shown in the following tables. For the four sequences, the rate-quality diagrams are depicted in Fig. 4.1, 4.2, 4.3 and 4.4.

Table 4.1: Extracted rate points and the corresponding PSNR values, for "Bus" sequence.

Rate (*kbps*)	PSNR (*dB*)	
106.62	23.94	L1
458.32	27.40	L2
951.11	29.93	L3
1232.91	31.01	L4
1974.47	32.56	L5
2705.53	34.92	L6
3609.72	36.88	L7
4710.62	37.99	L8
5264.39	38.91	L9
5953.11	40.40	L10
6291.31	41.61	L11
6680.73	42.67	L12
7244.51	44.01	L13
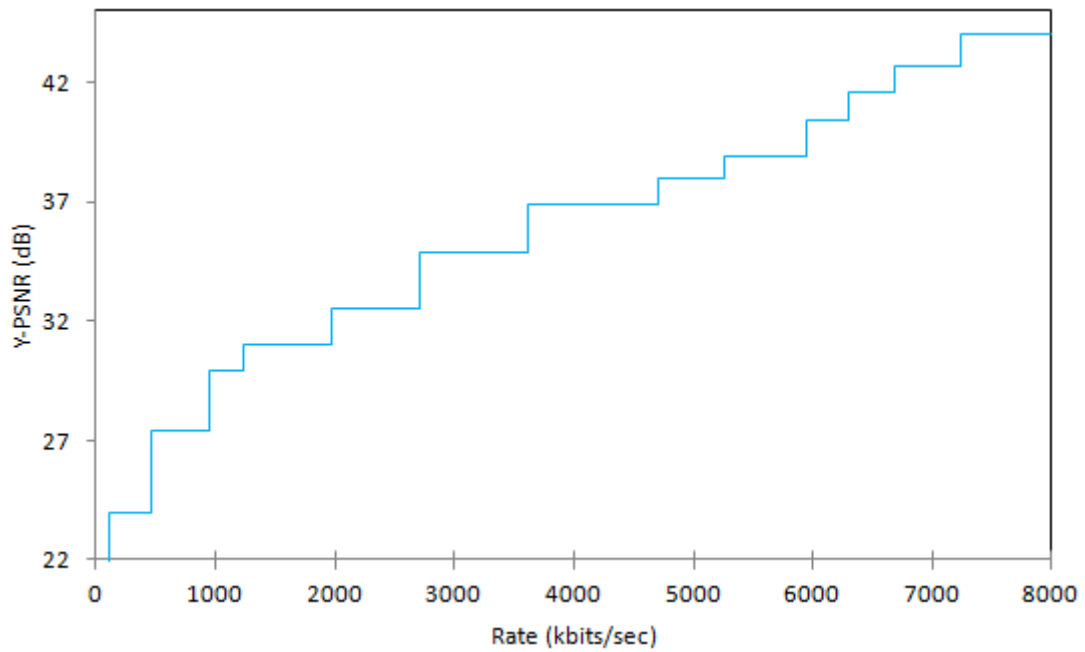
Figure 4.1: Quality-rate plot with MGS encoding for "Bus" sequence.

Table 4.2: Extracted rate points and the corresponding PSNR values, for "Foreman" sequence.

Rate (*kbps*)	PSNR (*dB*)	
42.92	26.84	L1
142.72	29.74	L2
268.90	30.70	L3
444.41	32.28	L4
705.91	33.31	L5
950.07	34.03	L6
1291.35	35.22	L7
1600.84	36.67	L8
2598.43	38.31	L9
3381.78	39.39	L10
3906.10	40.11	L11
4729.34	43.10	L12
5194.01	44.32	L13
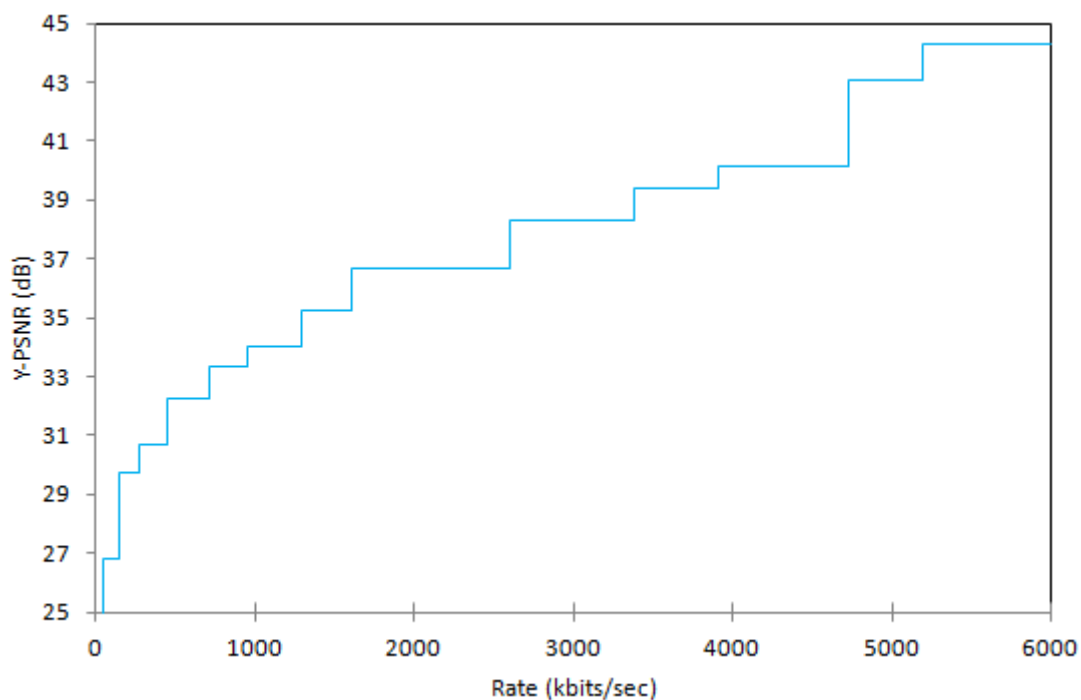
Figure 4.2: Quality-rate plot with MGS encoding for "Foreman" sequence.

Table 4.3: Extracted rate points and the corresponding PSNR values, for "Coastguard" sequence.

Rate (*kbps*)	PSNR (*dB*)	
36.67	25.11	L1
148.02	27.45	L2
442.27	29.23	L3
744.37	31.43	L4
1279.99	32.24	L5
1646.74	33.14	L6
2095.74	34.11	L7
2482.53	36.16	L8
3389.07	37.00	L9
4602.94	38.44	L10
5296.32	40.42	L11
5999.37	42.50	L12
6607.88	43.93	L13
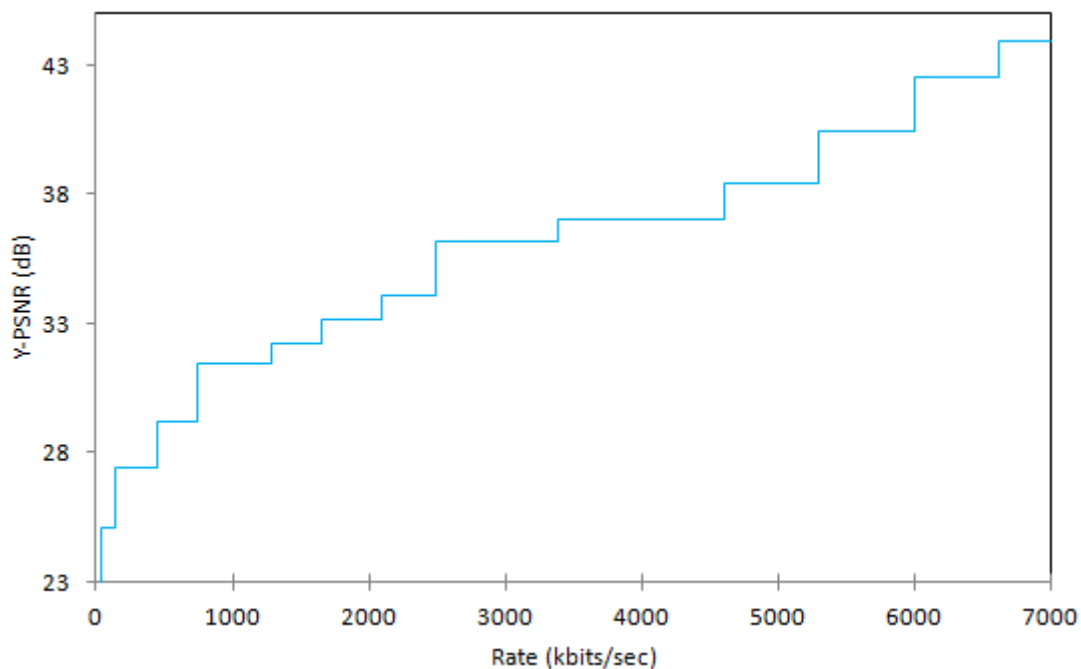
Figure 4.3: Quality-rate plot with MGS encoding for "Coastguard" sequence.

Table 4.4: Extracted rate points and the corresponding PSNR values, for "Akiyo" sequence.

Rate (*kbps*)	PSNR (*dB*)	
10.92	30.84	L1
51.12	34.86	L2
93.14	36.39	L3
139.50	39.07	L4
232.20	39.67	L5
299.21	41.27	L6
347.79	43.05	L7
589.44	43.24	L8
637.97	44.01	L9
761.62	44.71	L10
845.83	47.37	L11
874.69	47.70	L12
944.82	48.22	L13
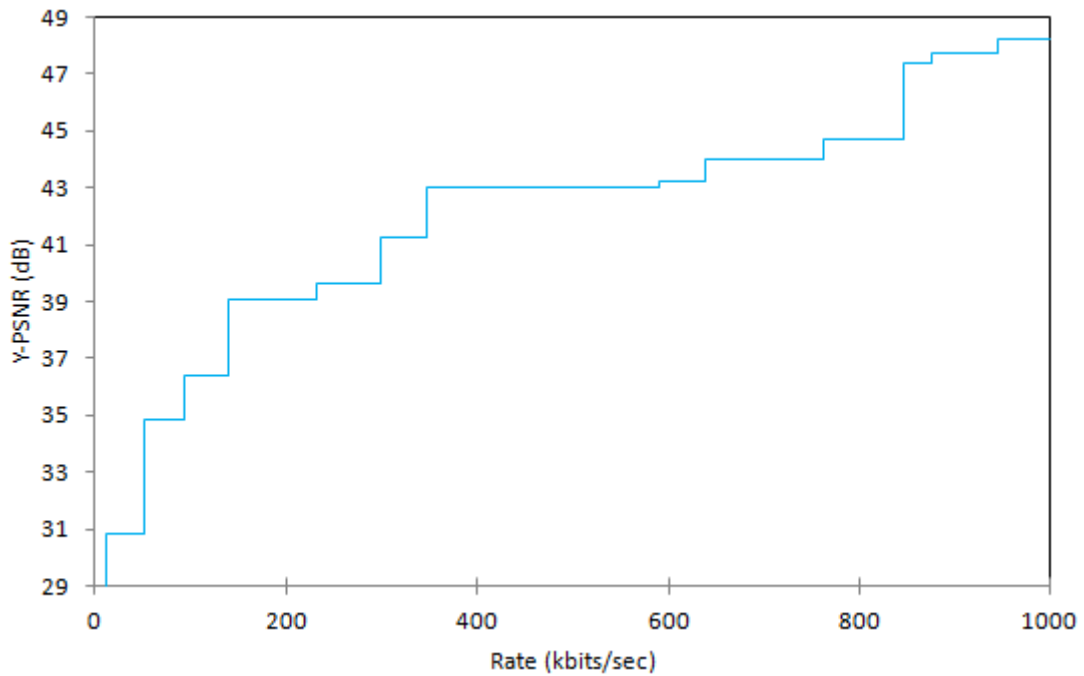
Figure 4.4: Quality-rate plot with MGS encoding for "Akiyo" sequence.

4.2 Efficiency and Fairness evaluation

The performance of the methods described in Chapter 3, was evaluated on the basis of efficiency and fairness criteria. Two metrics were used for the evaluation. The first one was the *Aggregate System Utility Index* (AUI), which is used in [8] and assesses the efficiency and the aggregate system utility. The second one is the *Jain's Index* (JI), which assesses the fairness of the resource allocation, defined as the minimization of video quality deviation among users who subscribe the same Quality of Service.

4.2.1 Aggregate Utility Index (AUI)

This metric examines the total utility that a scheme will bring cumulatively from all secondary users. According to *Aggregate Utility Index (AUI)* metric, the most efficient scheme is the one that gathers the highest overall system utility [31]. In our case, the utility is the received PSNR for each user, which is related to the video quality. We define the Aggregate Utility Index as,

$$AUI = \sum_{k=1}^{K} d_k. \tag{4.3}$$

4.2.2 Jain's Index (JI)

The *Jain's Index (JI)* metric expresses how close to a state of equality is a resource allocation scheme, and it is defined as,

$$JI = \frac{\left(\sum\limits_{k=1}^{K} L_k\right)^2}{K \sum\limits_{k=1}^{K} (L_k)^2}, \tag{4.4}$$

where L_k is the number of video layers that user k receives. JI takes values between 0 and 1. The closer its value is to 1, the more equal is the resource allocation scheme. This is the reason for employing this metric as a fairness estimator [31].

4.3 Simulation Results

In this section, we present the simulations cases along with the corresponding generated results. In each simulation instance, the two resource allocation methods described in Chapter 3, the Nash Bargaining Solution method (NBSm) and the Aggregate Visual Quality method (AVQm), were applied and compared in terms of efficiency and fairness. For each experiment, the Aggregate Utility Index (AUI) and the Jain's Index (JI) has been calculated and presented. Since the NBS method is formulated in a game theoretic mathematical framework and considers the maximization of Nash product as optimality, it was expected that, by applying it, fairness (expressed by JI) would be attained among

secondary users. Correspondingly, since AVQ method considers the maximization of aggregate PSNR as optimality, AVQm was expected to prevail in terms of efficiency (expressed by AUI).

Regarding PSO, the swarm size and the number of iterations were estimated after preliminary experimentation for each simulation case, recording the best detected solution. The discrete parameters were allowed to take continuous values for the position and velocity update, although they were rounded to the nearest integer for the evaluation of the particle. Since PSO is a stochastic algorithm, for each problem instance we conducted 30 independent experiments.

4.3.1 Single Video Transmission

CNR effect on resource allocation performance

In this experiment series, all secondary users were receiving the same video sequence, the "Foreman" sequence, encoded using the settings described above. At first, we inquired the impact of Channel-to-Noise Ratio (CNR) on the resource allocation performance. The number of subcarriers was set to N=128. The following table reports the video PSNR value and the corresponding number of layers (in parenthesis) each user receives, for different values of CNR.

Table 4.5: PSNR and corresponding layer (in parenthesis) for each user and AUI, JI values (N=128, K=6, M=4), for different values of CNR, Single Video transmission.

	CNR=21 dB		CNR=23 dB		CNR=25 dB		CNR=27 dB		CNR=29 dB	
	NBSm	AVQm	NBSm	AVQm	NBSm	AVQm	NBSm	AVQm	NBSm	AVQm
SU1 (dB)	36.67 (8)	36.67 (8)	36.67 (8)	36.67 (8)	36.67 (8)	36.67 (8)	36.67 (8)	36.67 (8)	36.67 (8)	36.67 (8)
SU2 (dB)	35.22 (7)	34.03 (6)	36.67 (8)	36.67 (8)	36.67 (8)	36.67 (8)	36.67 (8)	36.67 (8)	36.67 (8)	36.67 (8)
SU3 (dB)	34.03 (6)	36.67 (8)	35.22 (7)	36.67 (8)	34.02 (6)	36.67 (8)	36.67 (8)	36.67 (8)	36.67 (8)	36.67 (8)
SU4 (dB)	36.67 (8)	36.67 (8)	35.22 (7)	36.67 (8)	36.67 (8)	36.67 (8)	35.22 (7)	36.67 (8)	36.67 (8)	38.31 (9)
SU5 (dB)	34.03 (6)	33.31 (5)	35.22 (7)	34.03 (6)	35.22 (7)	32.28 (4)	35.22 (7)	34.03 (6)	36.67 (8)	35.22 (7)
SU6 (dB)	35.22 (7)	35.22 (7)	34.03 (6)	34.03 (6)	35.22 (7)	36.67 (8)	36.67 (8)	36.67 (8)	36.67 (8)	36.67 (8)
AUI (dB)	**211.84**	**212.57**	**213.03**	**214.74**	**215.21**	**215.63**	**217.12**	**217.38**	**220.02**	**220.21**
JI	**0.9866**	**0.9735**	**0.9909**	**0.9837**	**0.9898**	**0.9603**	**0.9962**	**0.9906**	**1.0000**	**0.9948**

Table (4.5) depicts that as CNR increases, which corresponds to channel conditions improvement, Aggregate Utility Index increases as well, for both NBSm and AVQm, implying efficiency improvement. This was expected because as the channel conditions improve, the probability of supporting more bits on each subcarrier increases as well. In the vast majority of the simulation experimental instances, the AVQm prevailed in terms

of efficiency, but performed inferiorly in terms of fairness, as for this method the Jain's Index values were smaller compared to the NBSm ones.

Efficiency and Fairness Performance for different number of secondary users

In the following tables the PSNR for each secondary user and the AUI, JI values after the optimal resource allocation for each method, are presented. All secondary users were receiving the same video sequence, the "Bus" sequence, encoded using the settings described above. Due to the fact that the channel fading between users and channels was modelled as an independent and identically distributed complex Gaussian, we performed several simulation instances for each case, setting CNR=25 dB. In each table four instances are reported.

Table 4.6: PSNR and corresponding layer (in parenthesis) for each user and AUI, JI values for four experiment instances (K=2, M=4), Single Video transmission.

	Instance 1		Instance 2		Instance 3		Instance 4	
	NBSm	AVQm	NBSm	AVQm	NBSm	AVQm	NBSm	AVQm
SU1 (dB)	34.92 (6)	34.92 (6)	36.88 (7)	36.88 (7)	36.88 (7)	36.88 (7)	34.92 (6)	34.92 (6)
SU2 (dB)	34.92 (6)	34.92 (6)	36.88 (7)	36.88 (7)	34.92 (6)	34.92 (6)	34.92 (6)	34.92 (6)
AUI (dB)	**69.84**	**69.84**	**73.76**	**73.76**	**71.8**	**71.8**	**69.84**	**69.84**
JI	**1.0000**	**1.0000**	**1.0000**	**1.0000**	**0.9941**	**0.9941**	**1.0000**	**1.0000**

Table 4.7: PSNR and corresponding layer (in parenthesis) for each user and AUI, JI values for four experiment instances (K=3, M=4), Single Video transmission.

	Instance 1		Instance 2		Instance 3		Instance 4	
	NBSm	AVQm	NBSm	AVQm	NBSm	AVQm	NBSm	AVQm
SU1 (dB)	32.56 (5)	31.01 (4)	32.56 (5)	31.01 (4)	31.01 (4)	31.01 (4)	32.56 (5)	32.56 (5)
SU2 (dB)	32.56 (5)	34.92 (6)	32.56 (5)	34.92 (6)	34.92 (6)	34.92 (6)	34.92 (6)	36.88 (7)
SU3 (dB)	31.01 (4)	31.01 (4)	34.92 (6)	34.92 (6)	34.92 (6)	36.88 (7)	31.01 (4)	31.01 (4)
AUI (dB)	**96.13**	**96.94**	**100.04**	**100.85**	**100.85**	**102.81**	**98.49**	**100.45**
JI	**0.9899**	**0.9607**	**0.9922**	**0.9697**	**0.9697**	**0.9538**	**0.9740**	**0.9481**

Table 4.8: PSNR and corresponding layer (in parenthesis) for each user and AUI, JI values for four experiment instances (K=4, M=4), Single Video transmission.

	Instance 1		Instance 2		Instance 3		Instance 4	
	NBSm	AVQm	NBSm	AVQm	NBSm	AVQm	NBSm	AVQm
SU1 (dB)	31.01 (4)	31.01 (4)	31.01 (4)	32.56 (5)	31.01 (4)	31.01 (4)	31.01 (4)	31.01 (4)
SU2 (dB)	32.56 (5)	31.01 (4)	31.01 (4)	31.01 (4)	32.56 (5)	31.01 (4)	32.56 (5)	31.01 (4)
SU3 (dB)	32.56 (5)	31.01 (4)	32.56 (5)	31.01 (4)	32.56 (5)	34.92 (6)	32.56 (5)	31.01 (4)
SU4 (dB)	31.01 (4)	34.92 (6)	31.01 (4)	31.01 (4)	31.01 (4)	31.01 (4)	31.01 (4)	34.92 (6)
AUI (dB)	**127.14**	**127.95**	**125.59**	**125.59**	**127.14**	**127.95**	**127.14**	**127.95**
JI	**0.9878**	**0.9304**	**0.9897**	**0.9897**	**0.9878**	**0.9304**	**0.9878**	**0.9304**

Table 4.9: PSNR and corresponding layer (in parenthesis) for each user and AUI, JI values for four experiment instances (K=5, M=4), Single Video transmission.

	Instance 1		Instance 2		Instance 3		Instance 4	
	NBSm	AVQm	NBSm	AVQm	NBSm	AVQm	NBSm	AVQm
SU1 (dB)	31.01 (4)	31.01 (4)	31.01 (4)	31.01 (4)	31.01 (4)	31.01 (4)	31.01 (4)	31.01 (4)
SU2 (dB)	31.01 (4)	31.01 (4)	31.01 (4)	31.01 (4)	31.01 (4)	32.56 (5)	31.01 (4)	31.01 (4)
SU3 (dB)	31.01 (4)	31.01 (4)	31.01 (4)	29.93 (3)	32.56 (5)	31.01 (4)	31.01 (4)	29.93 (3)
SU4 (dB)	32.56 (5)	34.92 (6)	31.01 (4)	32.56 (5)	32.56 (5)	34.92 (6)	31.01 (4)	32.56 (5)
SU5 (dB)	31.01 (4)	31.01 (4)	31.01 (4)	31.01 (4)	31.01 (4)	31.01 (4)	31.01 (4)	32.56 (5)
AUI (dB)	**156.6**	**158.96**	**155.05**	**155.52**	**158.15**	**160.51**	**155.05**	**157.07**
JI	**0.9897**	**0.9680**	**1.0000**	**0.97561**	**0.9878**	**0.9706**	**1.0000**	**0.9692**

Table 4.10: PSNR and corresponding layer (in parenthesis) for each user and AUI, JI values for four experiment instances (K=6, M=4), Single Video transmission.

	Instance 1		Instance 2		Instance 3		Instance 4	
	NBSm	AVQm	NBSm	AVQm	NBSm	AVQm	NBSm	AVQm
SU1 (dB)	29.93 (3)	31.01 (4)	31.01 (4)	32.56 (5)	29.93 (3)	31.01 (4)	31.01 (4)	31.01 (4)
SU2 (dB)	29.93 (3)	27.40 (2)	31.01 (4)	29.93 (3)	31.01 (4)	29.93 (3)	31.01 (4)	31.01 (4)
SU3 (dB)	29.93 (3)	32.56 (5)	29.93 (3)	31.01 (4)	31.01 (4)	31.01 (4)	31.01 (4)	31.01 (4)
SU4 (dB)	31.01 (4)	32.56 (5)	31.01 (4)	29.93 (3)	31.01 (4)	31.01 (4)	31.01 (4)	32.56 (5)
SU5 (dB)	31.01 (4)	29.93 (3)	31.01 (4)	31.01 (4)	29.93 (3)	31.01 (4)	29.93 (3)	29.93 (3)
SU6 (dB)	31.01 (4)	31.01 (4)	29.93 (3)	29.93 (3)	31.01 (4)	31.01 (4)	31.01 (4)	29.93 (3)
AUI (dB)	**182.82**	**184.47**	**183.9**	**184.37**	**183.9**	**184.98**	**184.98**	**185.45**
JI	**0.9800**	**0.9280**	**0.9837**	**0.9603**	**0.9906**	**0.9795**	**0.9906**	**0.9688**

Table 4.11: PSNR and corresponding layer (in parenthesis) for each user and AUI, JI values for four experiment instances (K=7, M=4), Single Video transmission.

	Instance 1		Instance 2		Instance 3		Instance 4	
	NBSm	AVQm	NBSm	AVQm	NBSm	AVQm	NBSm	AVQm
SU1 (dB)	29.93 (3)	31.01 (4)	29.93 (3)	31.01 (4)	31.01 (4)	27.40 (2)	27.40 (2)	27.40 (2)
SU2 (dB)	29.93 (3)	27.40 (2)	29.93 (3)	27.40 (3)	27.40 (3)	29.93 (2)	31.01 (4)	29.93 (2)
SU3 (dB)	29.93 (3)	31.01 (4)	29.93 (3)	31.01 (4)	29.93 (3)	32.56 (5)	29.93 (3)	29.93 (3)
SU4 (dB)	29.93 (3)	31.01 (4)	31.01 (4)	31.01 (4)	31.01 (4)	29.93 (3)	31.01 (4)	32.56 (5)
SU5 (dB)	29.93 (3)	29.93 (3)	29.93 (3)	29.93 (3)	29.93 (3)	31.01 (4)	27.40 (2)	27.40 (2)
SU6 (dB)	29.93 (3)	29.93 (3)	29.93 (3)	31.01 (4)	29.93 (3)	31.01 (4)	29.93 (3)	29.93 (3)
SU7 (dB)	27.40 (2)	27.40 (2)	29.93 (3)	29.93 (3)	31.01 (4)	29.93 (3)	29.93 (3)	31.01 (4)
AUI (dB)	**206.98**	**207.69**	**210.59**	**211.3**	**210.22**	**211.77**	**206.61**	**208.16**
JI	**0.9852**	**0.9344**	**0.9878**	**0.9568**	**0.9566**	**0.9351**	**0.9403**	**0.9098**

Table 4.12: PSNR and corresponding layer (in parenthesis) for each user and AUI, JI values for four experiment instances (K=8, M=4), Single Video transmission.

	Instance 1		Instance 2		Instance 3		Instance 4	
	NBSm	AVQm	NBSm	AVQm	NBSm	AVQm	NBSm	AVQm
SU1 (dB)	29.93 (3)	27.40 (2)	31.01 (4)	29.93 (3)	31.01 (4)	29.93 (3)	27.40 (2)	27.40 (2)
SU2 (dB)	29.93 (3)	31.01 (4)	27.40 (2)	27.40 (2)	27.40 (2)	27.40 (2)	27.40 (2)	27.40 (2)
SU3 (dB)	29.93 (3)	31.01 (4)	27.40 (2)	31.01 (4)	27.40 (2)	29.93 (3)	29.93 (3)	31.01 (4)
SU4 (dB)	29.93 (3)	29.93 (3)	31.01 (4)	31.01 (4)	29.93 (3)	29.93 (3)	29.93 (3)	29.93 (3)
SU5 (dB)	29.93 (3)	29.93 (3)	29.93 (3)	27.40 (2)	29.93 (3)	29.93 (3)	31.01 (4)	32.56 (5)
SU6 (dB)	27.40 (2)	27.40 (2)	27.40 (2)	27.40 (2)	27.40 (2)	29.93 (3)	29.93 (3)	31.01 (4)
SU7 (dB)	29.93 (3)	29.93 (3)	29.93 (3)	31.01 (4)	31.01 (4)	29.93 (3)	29.93 (3)	27.40 (2)
SU8 (dB)	29.93 (3)	31.01 (4)	29.93 (3)	31.01 (4)	29.93 (3)	27.40 (2)	29.93 (3)	29.93 (3)
AUI (dB)	**236.91**	**237.62**	**234.01**	**236.17**	**234.01**	**234.38**	**235.46**	**236.64**
JI	**0.9869**	**0.9413**	**0.9313**	**0.9191**	**0.9474**	**0.9231**	**0.9583**	**0.9191**

Table 4.13: PSNR and corresponding layer (in parenthesis) for each user and AUI, JI values for four experiment instances (K=9, M=4), Single Video transmission.

	Instance 1		Instance 2		Instance 3		Instance 4	
	NBSm	AVQm	NBSm	AVQm	NBSm	AVQm	NBSm	AVQm
SU1 (dB)	27.40 (2)	27.40 (2)	31.01 (4)	31.01 (4)	29.93 (3)	31.01 (4)	27.40 (2)	27.40 (2)
SU2 (dB)	27.40 (2)	31.01 (4)	29.93 (3)	29.93 (3)	27.40 (2)	27.40 (2)	27.40 (2)	27.40 (2)
SU3 (dB)	27.40 (2)	29.93 (3)	29.93 (3)	27.40 (2)	27.40 (2)	27.40 (2)	27.40 (2)	27.40 (2)
SU4 (dB)	29.93 (3)	31.01 (4)	27.40 (2)	27.40 (2)	27.40 (2)	27.40 (2)	27.40 (2)	27.40 (2)
SU5 (dB)	31.01 (4)	27.40 (2)	29.93 (3)	29.93 (3)	29.93 (3)	27.40 (2)	31.01 (4)	31.01 (4)
SU6 (dB)	29.93 (3)	27.40 (2)	27.40 (2)	27.40 (2)	29.93 (3)	27.40 (2)	27.40 (2)	27.40 (2)
SU7 (dB)	27.40 (2)	27.40 (2)	29.93 (3)	29.93 (3)	29.93 (3)	29.93 (3)	27.40 (2)	27.40 (2)
SU8 (dB)	27.40 (2)	27.40 (2)	27.40 (2)	27.40 (2)	27.40 (2)	29.93 (3)	27.40 (2)	27.40 (2)
SU9 (dB)	27.40 (2)	27.40 (2)	27.40 (2)	31.01 (4)	27.40 (2)	31.01 (4)	29.93 (3)	31.01 (4)
AUI (dB)	**255.27**	**256.35**	**260.33**	**261.41**	**256.72**	**258.88**	**252.74**	**253.82**
JI	**0.9272**	**0.9043**	**0.9412**	**0.9259**	**0.9603**	**0.9160**	**0.9245**	**0.8962**

In the following graphs the average Aggregate Utility Index (AUI) values and the Jain's Index (JI) values, for different number of secondary users $K = \{2, 3, ..., 9\}$, are depicted. The blue bars correspond to Nash Bargaining Solution resource allocation method, while the red bars to Aggregate Visual Quality method.
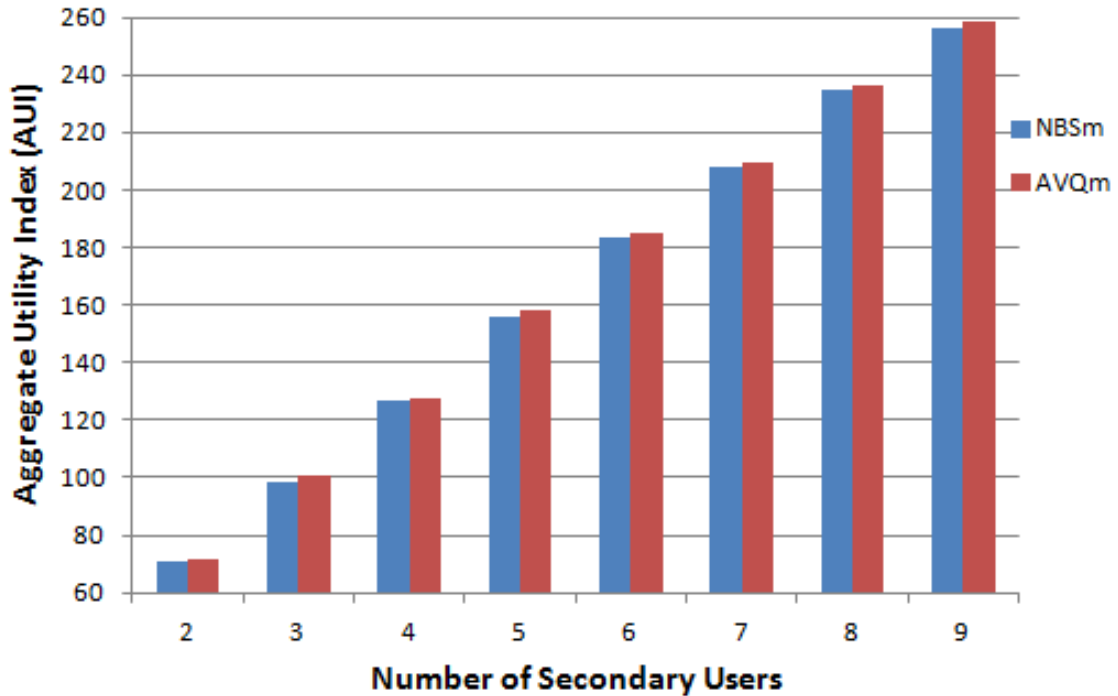
Figure 4.5: Average AUI values for different number of SU, Single Video transmission.
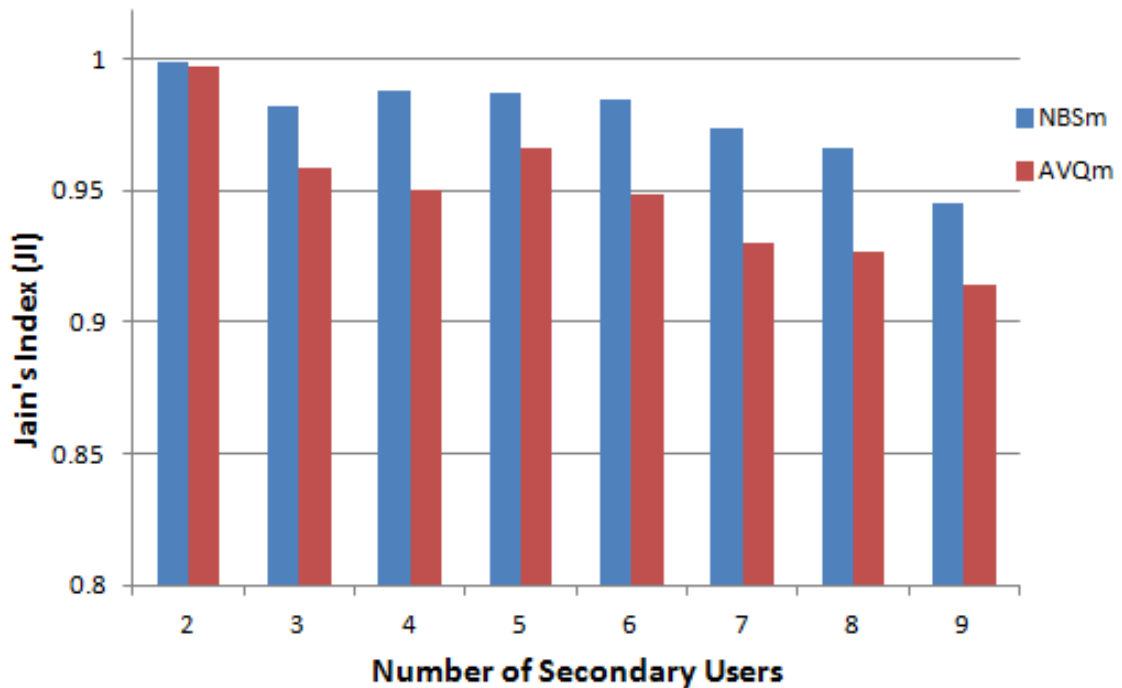
Figure 4.6: Average JI values for different number of SU, Single Video transmission.

The results of tables (4.6)-(4.13) and Figures 4.5 and 4.6 suggest that the AVQ method performed slightly better than the NBS method in terms of efficiency, as the AUI received higher values in all instances. This result was anticipated because the AVQ method considers the maximization of the aggregate visual quality as optimality measure. On the other hand, in the vast majority of the experimental results there was a distinct superiority of the NBS method over the AVQ method in terms of fairness, as dictated by the significantly greater values of the JI metric in most problem instances. These significant observations are optically illustrated in Fig. 4.5 and Fig. 4.6, where the relative performance of both methods is depicted.

Nash Bargaining Solution resource allocation method with unequal bargaining powers

As explained in 3.2.1, *bargaining power* is a weighting factor that expresses the advantage of a secondary user over the others, in the bargaining procedure. When a secondary user has a higher bargaining power, the resource allocation process favours him over the others and when all secondary users have the same value of bargaining powers, then they are all considered equal to each other. The previous experiments were conducted considering all the secondary users equal to each other, having the same value of bargaining powers. We performed several simulations considering the case that some users were favoured over the others, thus they were assigned a higher bargaining power. Specifically we considered a system with M=4 antennas, N=64 subcarriers and K=6 secondary users, SU 1 and SU 6 had $bp_1 = bp_6 = 0.4$, while all the other users had bargaining powers equal to 0.05 (the sum of the bargaining powers equals to one). The "Foreman" video sequence was transmitted to each secondary user. We performed several simulations instances. For each instance, the resource allocation was performed with NBS method retaining the same fading channel and system settings, at first with equal bargaining powers and then with unequal bargaining powers. The following tables report the received PSNR for each secondary user and the AUI values, for eight simulation instances.

Table 4.14: PSNR for each user and AUI values for NBS method, considering the cases of equal($bp_1 = bp_2 = bp_3 = bp_4 = bp_5 = bp_6 = 1/6$) and unequal ($bp_1 = bp_6 = 0.4$, $bp_2 = bp_3 = bp_4 = bp_5 = 0.05$) bargaining powers among the secondary users, K=6, M=4, Single Video transmission, experiment instances 1-4.

	Instance 1		Instance 2		Instance 3		Instance 4	
	Equal bp	Unequal bp	Equal bp	Unequal bp	Equal bp	Unequal bp	Equal bp	Unequal bp
SU1 (dB)	33.31	36.67	32.28	36.67	33.31	36.67	33.31	36.67
SU2 (dB)	32.28	29.74	32.28	29.74	32.28	29.74	32.28	30.70
SU3 (dB)	33.31	29.74	34.03	30.70	33.31	29.74	32.28	29.74
SU4 (dB)	32.28	29.74	33.31	29.74	33.31	29.74	33.31	32.28
SU5 (dB)	33.31	29.74	32.28	29.74	33.31	29.74	33.31	29.74
SU6 (dB)	32.28	34.03	32.28	34.03	32.28	35.22	33.31	35.22
AUI	**196.77**	**189.66**	**196.46**	**190.62**	**197.80**	**190.85**	**197.80**	**194.35**

Table 4.15: PSNR for each user and AUI values for NBS method, considering the cases of equal($bp_1 = bp_2 = bp_3 = bp_4 = bp_5 = bp_6 = 1/6$) and unequal ($bp_1 = bp_6 = 0.4$, $bp_2 = bp_3 = bp_4 = bp_5 = 0.05$) bargaining powers among the secondary users, K=6, M=4, Single Video transmission, experiment instances 5-8.

	Instance 5		Instance 6		Instance 7		Instance 8	
	Equal bp	Unequal bp	Equal bp	Unequal bp	Equal bp	Unequal bp	Equal bp	Unequal bp
SU1 (dB)	32.28	34.03	33.31	36.67	32.28	36.67	32.28	35.22
SU2 (dB)	32.28	30.70	32.28	29.74	33.31	30.70	32.28	30.70
SU3 (dB)	33.31	29.74	32.28	29.74	34.03	29.74	33.31	30.70
SU4 (dB)	33.31	30.70	33.31	30.70	33.31	29.74	33.31	29.74
SU5 (dB)	33.31	29.74	32.28	29.74	32.28	30.70	34.03	30.70
SU6 (dB)	32.28	36.67	33.31	36.67	32.28	36.67	32.28	35.22
AUI	**196.77**	**191.58**	**196.77**	**193.26**	**197.49**	**194.22**	**197.49**	**192.28**

The results, obviously, confirm the precedent theory. The first column of each instance, corresponding to equal bargaining powers case, reports the fairness attainment among all secondary users, considering them equal to each other. However, the second column,

corresponding to unequal bargaining powers, with bp_1 and bp_6 much larger than the other users' bp, depicts that SU1 and SU6 have been considered of higher prioritization and importance throughout the bargaining process. This assumption is generated by observing the PSNR values for these users; while SU1 and SU6, when considered equal to all the other users, have PSNR approximately of definitely equal to the other users', if they are considered favoured over the others, they attain a PSNR value higher, not only than the other users' PSNR, but also than the value they had in the equal bargaining power case. SU2, SU3, SU4 and SU5 in both cases are considered equal to each other and try to reach a mutually beneficial agreement on the resource allocation.

Another observation made from there tables, is that employing an unequal bargaining power scheme to favour some secondary users over the others, comes at the cost of the Aggregate Utility Index values' reduction, thus the overall efficiency performance of the system.

4.3.2 Multiple Videos Transmission

We performed a number of experiments, transmitting multiple videos to multiple secondary users. Specifically, we used three video sequences, the "Foreman","Coastguard" and "Akiyo" sequences, all encoded using the settings described above. Each user was receiving one predefined video sequence and the assignment was defined serially, i.e. the first user received "Foreman", the second "Coastguard", the third "Akiyo", the fourth "Foreman", the fifth "Coastguard", and so on. As mentioned above, the first two sequences ("Foreman" and "Coastguard") are high-motion while "Akiyo" is a low-motion sequence. This means that the PSNR values for low rate values are higher in "Akiyo", compared to the other two sequences, as depicted in Figures 4.4, 4.2 and 4.3. As a result, for the same rate, different video quality layer will be transmitted to each user, depending on the video sequence that it has been assigned to him. This explains the differences in PSNR values and corresponding layers in the following result tables.

CNR effect on resource allocation performance

We firstly inquired the impact of Channel-to-Noise Ratio (CNR) to the resource allocation performance. The number of subcarriers was set to $N=128$. The following table reports the video PSNR value and the corresponding number of layers (in parenthesis) each user receives, for different values of CNR.

Table 4.16: PSNR and corresponding layer (in parenthesis) for each user and AUI, JI values (N=128, K=6, M=4), for different values of CNR, Multiple Video transmission.

	CNR=21 dB		CNR=23 dB		CNR=25 dB		CNR=27 dB		CNR=29 dB	
	NBSm	AVQm	NBSm	AVQm	NBSm	AVQm	NBSm	AVQm	NBSm	AVQm
SU1 (dB)	33.31 (5)	34.03 (6)	34.03 (6)	34.03 (6)	34.03 (6)	36.67 (8)	36.67 (8)	36.67 (8)	36.67 (8)	36.67 (8)
SU2 (dB)	31.43 (4)	31.43 (4)	31.43 (4)	31.43 (4)	32.24 (5)	31.43 (4)	32.24 (5)	31.43 (4)	32.24 (5)	32.24 (5)
SU3 (dB)	47.70 (12)	48.22 (13)	47.70 (12)	48.22 (13)	47.70 (12)	48.22 (13)	47.70 (12)	48.22 (13)	47.70 (12)	48.22 (13)
SU4 (dB)	35.22 (7)	34.03 (6)	36.67 (8)	36.67 (8)	36.67 (8)	36.67 (8)	36.67 (8)	36.67 (8)	36.67 (8)	36.67 (8)
SU5 (dB)	31.43 (4)	31.43 (4)	32.24 (5)	31.43 (4)	32.24 (5)	31.43 (4)	32.24 (5)	31.43 (4)	33.14 (6)	32.24 (5)
SU6 (dB)	47.70 (12)	48.22 (13)	47.70 (12)	48.22 (13)	47.70 (12)	48.22 (13)	47.70 (12)	48.22 (13)	47.70 (12)	48.22 (13)
AUI (dB)	**226.79**	**227.36**	**229.77**	**230.00**	**230.58**	**232.64**	**233.22**	**232.64**	**234.12**	**234.26**
JI	**0.8190**	**0.7979**	**0.8582**	**0.8170**	**0.8767**	**0.8367**	**0.8941**	**0.8367**	**0.9088**	**0.8734**

The observations made in the single video transmission case, apply also in this case. As the channel conditions increase, the Aggregate Utility Index values increase as well. The AUI metric confirmed that the AVQ method performed better in terms of efficiency (greater AUI values), while JI metric proved that NBS method provided better results in terms of fairness (greater JI values).

Efficiency and Fairness Performance for different number of secondary users

In the following tables the PSNR for each secondary user and the AUI, JI values after the optimal resource allocation for each method, are presented. Due to the fact that the channel fading between users and channels was modelled as an independent and identically distributed complex Gaussian, we performed several simulation instances for each case, setting CNR=25 dB and N=64 subcarriers. In each table four instances are reported.

Table 4.17: PSNR and corresponding layer (in parenthesis) for each user and AUI, JI values for four experiment instances (K=3, M=4), Multiple Video transmission.

	Instance 1		Instance 2		Instance 3		Instance 4	
	NBSm	AVQm	NBSm	AVQm	NBSm	AVQm	NBSm	AVQm
SU1 (dB)	32.28 (4)	32.28 (4)	32.28 (4)	30.70 (3)	30.70 (3)	32.28 (4)	33.31 (5)	32.28 (4)
SU2 (dB)	31.43 (4)	27.45 (2)	29.23 (3)	27.45 (2)	31.43 (4)	27.45 (2)	29.23 (3)	27.45 (2)
SU3 (dB)	43.05 (7)	48.22 (13)	43.05 (7)	48.22 (13)	43.05 (7)	47.70 (12)	43.05 (7)	48.22 (13)
AUI (dB)	**106.76**	**107.95**	**104.56**	**106.37**	**105.18**	**107.43**	**105.59**	**107.95**
JI	**0.9259**	**0.6367**	**0.8829**	**0.5934**	**0.8829**	**0.6585**	**0.9036**	**0.6367**

Table 4.18: PSNR and corresponding layer (in parenthesis) for each user and AUI, JI values for four experiment instances (K=4, M=4), Multiple Video transmission.

	Instance 1		Instance 2		Instance 3		Instance 4	
	NBSm	AVQm	NBSm	AVQm	NBSm	AVQm	NBSm	AVQm
SU1 (dB)	32.28 (4)	30.70 (3)	32.28 (4)	30.70 (3)	30.70 (3)	32.28 (4)	30.70 (3)	29.74 (2)
SU2 (dB)	29.23 (3)	27.45 (2)	27.45 (2)	27.45 (2)	29.23 (3)	27.45 (2)	29.23 (3)	27.45 (2)
SU3 (dB)	43.05 (7)	47.70 (12)	43.05 (7)	48.22 (13)	43.05 (7)	47.70 (12)	43.05 (7)	47.70 (12)
SU4 (dB)	30.70 (3)	30.70 (3)	32.28 (4)	30.70 (3)	32.28 (4)	32.28 (4)	32.28 (4)	30.70 (3)
AUI (dB)	**135.26**	**136.55**	**135.06**	**137.07**	**135.26**	**139.71**	**135.26**	**135.59**
JI	**0.8705**	**0.6024**	**0.8500**	**0.6024**	**0.8705**	**0.6722**	**0.8705**	**0.5606**

Table 4.19: PSNR and corresponding layer (in parenthesis) for each user and AUI, JI values for four experiment instances (K=5, M=4), Multiple Video transmission.

	Instance 1		Instance 2		Instance 3		Instance 4	
	NBSm	AVQm	NBSm	AVQm	NBSm	AVQm	NBSm	AVQm
SU1 (dB)	32.28 (4)	29.74 (2)	32.28 (4)	30.70 (3)	29.74 (2)	29.74 (2)	30.70 (3)	29.74 (2)
SU2 (dB)	27.45 (2)	27.45 (2)	27.45 (2)	27.45 (2)	29.23 (3)	27.45 (2)	29.23 (3)	27.45 (2)
SU3 (dB)	43.05 (7)	47.70 (12)	43.05 (7)	47.70 (12)	43.05 (7)	47.70 (12)	43.05 (7)	47.70 (12)
SU4 (dB)	32.28 (4)	30.70 (3)	32.28 (4)	30.70 (3)	32.28 (4)	30.70 (3)	32.28 (4)	30.70 (3)
SU5 (dB)	27.45 (2)	27.45 (2)	27.45 (2)	27.45 (2)	27.45 (2)	27.45 (2)	27.45 (2)	27.45 (2)
AUI (dB)	**162.51**	**163.04**	**162.51**	**164.00**	**161.75**	**163.04**	**162.71**	**163.04**
JI	**0.8112**	**0.5345**	**0.8112**	**0.5694**	**0.7902**	**0.5345**	**0.8299**	**0.5345**

Table 4.20: PSNR and corresponding layer (in parenthesis) for each user and AUI, JI values for four experiment instances (K=6, M=4), Multiple Video transmission.

	Instance 1		Instance 2		Instance 3		Instance 4	
	NBSm	AVQm	NBSm	AVQm	NBSm	AVQm	NBSm	AVQm
SU1 (dB)	30.70 (3)	29.74 (2)	30.70 (3)	30.70 (3)	32.28 (4)	32.28 (4)	30.70 (3)	30.70 (3)
SU2 (dB)	27.45 (2)	27.45 (2)	27.45 (2)	27.45 (2)	27.45 (2)	27.45 (2)	27.45 (2)	27.45 (2)
SU3 (dB)	43.05 (7)	43.05 (7)	39.07 (4)	43.05 (7)	39.07 (4)	43.05 (7)	39.07 (4)	43.05 (7)
SU4 (dB)	30.70 (3)	30.70 (3)	30.70 (3)	29.74 (2)	32.28 (4)	29.74 (2)	30.70 (3)	30.70 (3)
SU5 (dB)	27.45 (2)	27.45 (2)	29.23 (3)	27.45 (2)	27.45 (2)	27.45 (2)	29.23 (3)	27.45 (2)
SU6 (dB)	39.07 (4)	43.05 (7)	43.05 (7)	43.05 (7)	43.05 (7)	43.05 (7)	43.05 (7)	43.05 (7)
AUI (dB)	**198.42**	**201.44**	**200.20**	**201.44**	**201.58**	**203.02**	**200.20**	**202.40**
JI	**0.8077**	**0.7409**	**0.8403**	**0.7409**	**0.8397**	**0.7619**	**0.8403**	**0.7742**

Table 4.21: PSNR and corresponding layer (in parenthesis) for each user and AUI, JI values for four experiment instances (K=7, M=4), Multiple Video transmission.

	Instance 1		Instance 2		Instance 3		Instance 4	
	NBSm	AVQm	NBSm	AVQm	NBSm	AVQm	NBSm	AVQm
SU1 (dB)	30.70 (3)	33.31 (5)	30.70 (3)	29.74 (2)	32.28 (4)	30.70 (3)	30.70 (3)	29.74 (2)
SU2 (dB)	27.45 (2)	27.45 (2)	27.45 (2)	27.45 (2)	27.45 (2)	27.45 (2)	27.45 (2)	27.45 (2)
SU3 (dB)	43.05 (7)	43.05 (7)	43.05 (7)	43.05 (7)	43.05 (7)	43.05 (7)	43.05 (7)	43.05 (7)
SU4 (dB)	30.70 (3)	29.74 (2)	30.70 (3)	29.74 (2)	29.74 (2)	29.74 (2)	29.74 (2)	29.74 (2)
SU5 (dB)	27.45 (2)	27.45 (2)	27.45 (2)	27.45 (2)	27.45 (2)	27.45 (2)	27.45 (2)	27.45 (2)
SU6 (dB)	39.07 (4)	43.05 (7)	39.07 (4)	43.05 (7)	39.07 (4)	43.05 (7)	43.05 (7)	43.05 (7)
SU7 (dB)	30.70 (3)	30.70 (3)	29.74 (2)	29.74 (2)	30.70 (3)	29.74 (2)	29.74 (2)	30.70 (3)
AUI (dB)	**229.12**	**234.75**	**228.16**	**230.22**	**229.74**	**231.18**	**231.18**	**231.18**
JI	**0.8229**	**0.7259**	**0.7955**	**0.6973**	**0.8067**	**0.7259**	**0.7259**	**0.7259**

Table 4.22: PSNR and corresponding layer (in parenthesis) for each user and AUI, JI values for four experiment instances (K=8, M=4), Multiple Video transmission.

	Instance 1		Instance 2		Instance 3		Instance 4	
	NBSm	AVQm	NBSm	AVQm	NBSm	AVQm	NBSm	AVQm
SU1 (dB)	30.70 (3)	29.74 (2)	29.74 (2)	29.74 (2)	29.74 (2)	29.74 (2)	30.70 (3)	29.74 (2)
SU2 (dB)	27.45 (2)	27.45 (2)	27.45 (2)	27.45 (2)	27.45 (2)	27.45 (2)	27.45 (2)	27.45 (2)
SU3 (dB)	39.07 (4)	43.05 (7)	43.05 (7)	43.05 (7)	39.07 (4)	43.05 (7)	39.07 (4)	41.27 (6)
SU4 (dB)	29.74 (2)	29.74 (2)	29.74 (2)	29.74 (2)	29.74 (2)	29.74 (2)	29.74 (2)	29.74 (2)
SU5 (dB)	27.45 (2)	27.45 (2)	27.45 (2)	25.11 (1)	27.45 (2)	27.45 (2)	27.45 (2)	25.11 (1)
SU6 (dB)	39.07 (4)	39.07 (4)	39.07 (4)	43.05 (7)	43.05 (7)	43.05 (7)	39.07 (4)	43.05 (7)
SU7 (dB)	30.70 (3)	29.74 (2)	30.70 (3)	29.74 (2)	29.74 (2)	29.74 (2)	30.70 (3)	29.74 (2)
SU8 (dB)	27.45 (2)	25.11 (1)	27.45 (2)	27.45 (2)	27.45 (2)	25.11 (1)	27.45 (2)	25.11 (1)
SU9 (dB)	39.07 (4)	43.05 (7)	39.07 (4)	39.07 (4)	39.07 (4)	39.07 (4)	39.07 (4)	43.05 (7)
AUI (dB)	**290.70**	**294.40**	**293.72**	**294.40**	**292.76**	**294.40**	**290.70**	**294.26**
JI	**0.9160**	**0.6922**	**0.7919**	**0.6922**	**0.771429**	**0.692181**	**0.9160**	**0.6579**

Table 4.23: PSNR and corresponding layer (in parenthesis) for each user and AUI, JI values for four experiment instances (K=9, M=4), Multiple Video transmission.

	Instance 1		Instance 2		Instance 3		Instance 4	
	NBSm	AVQm	NBSm	AVQm	NBSm	AVQm	NBSm	AVQm
SU1 (dB)	27.40 (2)	27.40 (2)	31.01 (4)	31.01 (4)	29.93 (3)	31.01 (4)	27.40 (2)	27.40 (2)
SU2 (dB)	27.40 (2)	31.01 (4)	29.93 (3)	29.93 (3)	27.40 (2)	27.40 (2)	27.40 (2)	27.40 (2)
SU3 (dB)	27.40 (2)	29.93 (3)	29.93 (3)	27.40 (2)	27.40 (2)	27.40 (2)	27.40 (2)	27.40 (2)
SU4 (dB)	29.93 (3)	31.01 (4)	27.40 (2)	27.40 (2)	27.40 (2)	27.40 (2)	27.40 (2)	27.40 (2)
SU5 (dB)	31.01 (4)	27.40 (2)	29.93 (3)	29.93 (3)	29.93 (3)	27.40 (2)	31.01 (4)	31.01 (4)
SU6 (dB)	29.93 (3)	27.40 (2)	27.40 (2)	27.40 (2)	29.93 (3)	27.40 (2)	27.40 (2)	27.40 (2)
SU7 (dB)	27.40 (2)	27.40 (2)	29.93 (3)	29.93 (3)	29.93 (3)	29.93 (3)	27.40 (2)	27.40 (2)
SU8 (dB)	27.40 (2)	27.40 (2)	27.40 (2)	27.40 (2)	27.40 (2)	29.93 (3)	27.40 (2)	27.40 (2)
SU9 (dB)	27.40 (2)	27.40 (2)	27.40 (2)	31.01 (4)	27.40 (2)	31.01 (4)	29.93 (3)	31.01 (4)
AUI (dB)	**255.27**	**256.35**	**260.33**	**261.41**	**256.72**	**258.88**	**252.74**	**253.82**
JI	**0.9272**	**0.9043**	**0.9412**	**0.9259**	**0.9603**	**0.9160**	**0.9245**	**0.8962**

In the following graphs the average Aggregate Utility Index (AUI) values and the Jain's Index (JI) values, for different number of secondary users $K = \{3, ..., 9\}$, are depicted. The blue bars correspond to Nash Bargaining Solution resource allocation method, while the red bars to Aggregate Visual Quality method.
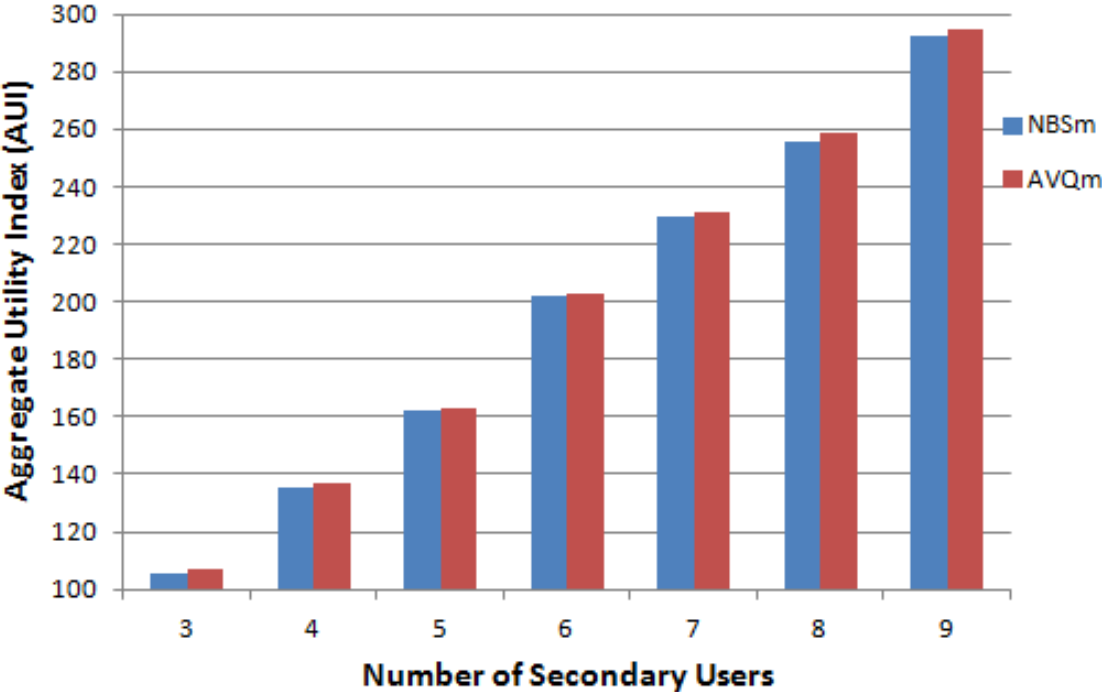

Figure 4.7: Average AUI values for different number of SU, Multiple Video transmission.
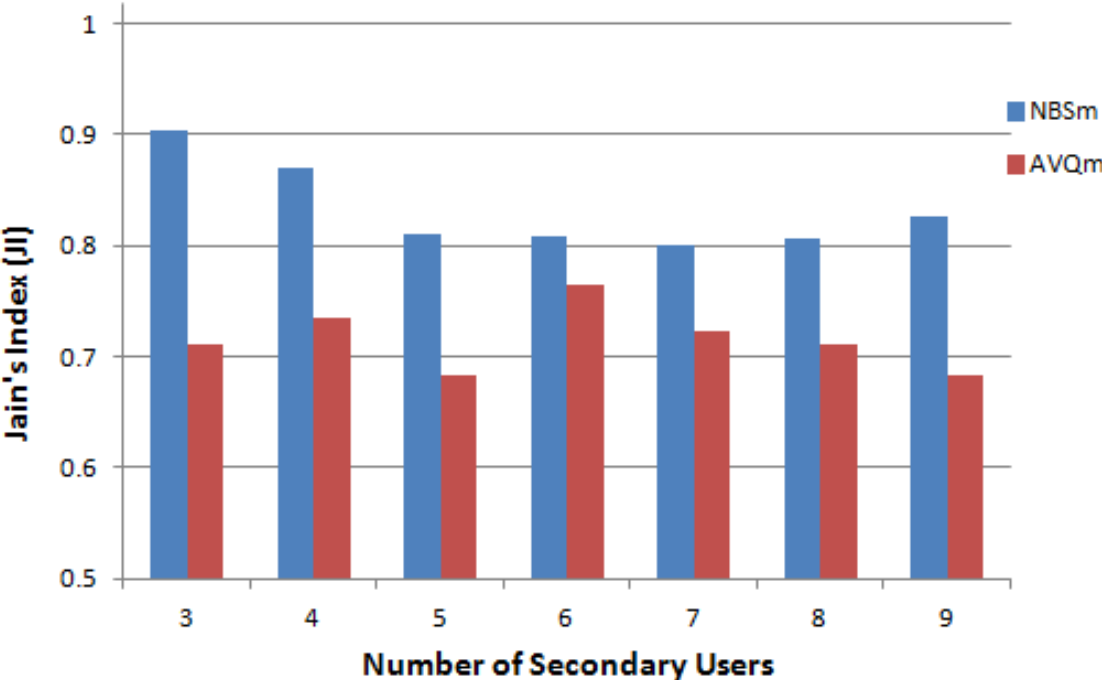

Figure 4.8: Average JI values for different number of SU, Multiple Video transmission.

The results of tables (4.17)-(4.23) and Figures 4.7 and 4.8 confirm that the AVQ method performed slightly better than the NBS method in terms of efficiency, while in the vast majority of the experimental results there was a distinct superiority of the NBS method over the AVQ method in terms of fairness. These significant observations are depicted in Fig. 4.7 and Fig. 4.8, where the relative performance of both methods is reported.

Nash Bargaining Solution resource allocation method with unequal bargaining powers

Finally, we performed several simulations considering the case that some users were favoured over the others, thus they were assigned a higher bargaining power, when multiple videos sere transmitted. Specifically we considered a system with M=4 antennas, N=64 subcarriers and K=6 secondary users, SU 1 and SU 6 had $bp_1 = bp_6 = 0.4$, while all the other users had bargaining powers equal to 0.05. The "Foreman", "Coastguard" and "Akiyo" video sequences were transmitted to the secondary users, the same way as in previous experiments, i.e. SU 1 and SU 4 receive "Foreman" sequence, SU 2 and 5 receive "Coastguard" sequence, and finally SU 3 and SU 6 receive the "Akiyo" sequence. We performed several simulations instances. For each instance, the resource allocation was performed with NBS method retaining the same fading channel and system settings, at first with equal bargaining powers and then with unequal bargaining powers. The following tables report the received PSNR for each secondary user and the AUI values, for eight simulation instances.

Table 4.24: PSNR for each user and AUI values for NBS method, considering the cases of equal($bp_1 = bp_2 = bp_3 = bp_4 = bp_5 = bp_6 = 1/6$) and unequal ($bp_1 = bp_6 = 0.4$, $bp_2 = bp_3 = bp_4 = bp_5 = 0.05$) bargaining powers among the secondary users, K=6, M=4, Multiple Video transmission, experiment instances 1-4.

	Instance 1		Instance 2		Instance 3		Instance 4	
	Equal bp	Unequal bp	Equal bp	Unequal bp	Equal bp	Unequal bp	Equal bp	Unequal bp
SU1 (dB)	33.31	36.67	32.28	36.67	33.31	35.22	32.28	36.67
SU2 (dB)	31.43	27.45	31.43	27.45	31.43	27.45	31.43	29.23
SU3 (dB)	43.05	43.05	43.05	39.07	43.05	43.05	47.70	43.05
SU4 (dB)	32.28	30.70	33.31	29.74	32.28	30.70	32.28	29.74
SU5 (dB)	31.43	27.45	31.43	27.45	31.43	27.45	31.43	27.45
SU6 (dB)	43.05	48.22	43.05	47.37	43.05	48.22	43.05	48.22
AUI	**214.55**	**213.54**	**214.55**	**207.75**	**214.55**	**212.09**	**218.17**	**214.36**

Table 4.25: PSNR for each user and AUI values for NBS method, considering the cases of equal($bp_1 = bp_2 = bp_3 = bp_4 = bp_5 = bp_6 = 1/6$) and unequal ($bp_1 = bp_6 = 0.4$, $bp_2 = bp_3 = bp_4 = bp_5 = 0.05$) bargaining powers among the secondary users, K=6, M=4, Multiple Video transmission, experiment instances 5-8.

	Instance 5		Instance 6		Instance 7		Instance 8	
	Equal bp	Unequal bp	Equal bp	Unequal bp	Equal bp	Unequal bp	Equal bp	Unequal bp
SU1 (dB)	32.28	36.67	32.28	34.03	32.28	35.22	32.28	34.03
SU2 (dB)	31.43	27.45	31.43	27.45	31.43	27.45	31.43	29.23
SU3 (dB)	47.37	39.07	43.05	43.05	43.05	39.07	43.05	43.05
SU4 (dB)	32.28	30.70	33.31	32.28	32.28	30.70	32.28	30.70
SU5 (dB)	31.43	27.45	31.43	27.45	31.43	27.45	31.43	27.45
SU6 (dB)	43.05	48.22	43.05	48.22	43.24	48.22	43.05	48.22
AUI	**217.84**	**209.56**	**214.55**	**212.48**	**213.71**	**208.11**	**213.52**	**212.68**

The assumptions made for the Single Video transmission, apply to the Multiple Video transmission as well. The first column of each instance, which corresponds to the equal bargaining powers case, reports the fairness attainment among all secondary users, considering them equal to each other. On the other hand, the second column, corresponding to unequal bargaining powers, with bp_1 and bp_6 much larger than the other users' bp, depicts that SU1 and SU6 have been considered of higher prioritization and importance throughout the bargaining process. This assumption is generated by observing the PSNR values for these users; while SU1 and SU6, when considered equal to all the other users, have PSNR approximately of definitely equal to the other users', if they are considered favoured over the others, they attain a PSNR value higher, not only than the other users' PSNR, but also than the value they had in the equal bargaining power case. SU2, SU3, SU4 and SU5 in both cases are considered equal to each other and try to reach a mutually beneficial agreement on the resource allocation.

Finally, employing an unequal bargaining power scheme to favour some secondary users over the others, comes to the cost of the Aggregate Utility Index values' reduction, thus the overall efficiency performance of the system.

CHAPTER 5

CONCLUSIONS AND FUTURE WORK

5.1 Conclusions

5.2 Future work

5.1 Conclusions

In the present thesis, we proposed a game-theoretic resource allocation method for transmitting video sequences among multiple users, over a multiple-input-single-output (MISO) cognitive radio network. A basic consideration for this method was its ability perform effectively in terms of two essential service objectives: fairness and efficiency. Fairness concerned the video quality deviation among users who subscribe the same quality of service, while efficiency relates to how to attain the highest overall video quality using the available system resources.

The cognitive base station of the CR network was equipped with multiple transmit antennas, as the superiority of MIMO cognitive radio systems over single antenna cognitive systems in terms of throughput improvement and interference limitations, has been widely researched and confirmed. The transmitted video sequences were encoded using the Medium-grain quality scalability (MGS) scheme of Scalable Video Coding (SVC) extension of the H.264/AVC standard, which enables the adaptation of the video coding process to the bandwidth restrictions and channel conditions fluctuations.

After setting up the system model characteristics, we introduced a game-theoretic Nash Bargaining Solution framework, to explore fairness attribution to subscribed secondary users. Moreover, a method based on maximizing the aggregate visual quality of secondary users was implemented to compare and evaluate the results. We transformed the two methods of resource allocation to two optimization problems; in the first method the objective was the maximization of Nash product of the secondary users, whilst in the second the objective was the maximization of aggregate visual quality. In both methods,

the formulated optimization problems were taking into consideration the minimization of resources waste, an issue which was provoked by the staircase quality-rate characteristic of MGS coding scheme.

To solve each optimization problem we employed the PSO algorithm, which belongs to swarm intelligence optimization methods. Because of the problem high dimensionality we introduced a method of reducing it, by exploiting the system features. Regarding the results evaluation, we used two metrics to assess our approach: one to evaluate efficiency (Aggregate Utility Index) and another to evaluate fairness (Jain's Index).

We performed several experiments for both methods, simulating the aforementioned system model, and the results were evaluated. We examined two cases: the first one was the case of single video transmission to all the secondary users and the other one was the case of multiple video transmission, where the three different transmitted videos had different motion characteristics. Over all systems settings and scenarios, the experiments reported the superiority of the proposed NBS method in terms of fairness among the secondary users, over the AVQ method. However, as it was expected, the second method performed better in terms of efficiency, as it was formulated upon an aggregate visual quality maximization framework. Nevertheless, the efficiency performance difference was slight; this fact, combined with the NBS method's enhanced fairness attribution, proves that the proposed method can provide notably efficient and fairer allocation solutions against the AVQ method.

Moreover, the results showed that as the CNR increases, thus the channel conditions enhance, the efficiency of both methods increases as well. Finally, we performed simulations for the NBS method to investigate the system's performance when unequal bargaining powers are assigned to the secondary users, during the bargaining game procedure. We set higher values of bargaining power for several users and the remaining users' bargaining powers were considered equal to each other. The results confirmed what Nash claimed; these several users were favoured in the bargaining game, as the video quality they attained was higher compared not only to the quality level the other users attained, but also to the quality level they would achieve considering the case of equal bargaining powers among all users. This feature of the NBS method could be applied for setting user prioritization rules or to cope with different user requirements.

5.2   Future work

In section 5.1 we presented the scope of the present work. Since the proposed framework consists of several schemes and parameters settings, there can be some directions for future work.

Firstly, as far as the system model is concerned, several channel coding schemes could be employed and its contribution to throughput enhancing could be investigated. It should be noted that in this case, a table for different modulation and coding schemes would be used instead of equations (3.5) and (3.6).

Apart from that, instead of using exclusively the MGS quality scalability of H.264 SVC standard, and since modern telecommunications demand the video transmission to portable devices that support different spatial resolutions, spatial scalability or combined scalability modalities could be taken into consideration for future work. The minimization of service deviation among secondary users or the correspondence to different user requirements is of great importance in such systems.

Further enquiry in objective function formulation could be also performed. Since NBSm contributes to fairness attainment and AVQm performs slightly better in terms of efficiency, an objective function that would maximize the Nash product along with the aggregate visual quality with the employment of corresponding weighting factors, while minimizing the resources waste, could be formulated.

BIBLIOGRAPHY

[1] S. Haykin, Cognitive Radio: Brain-Empowered Wireless Communications, *IEEE Journal on selected areas in Communications* **23** (2005) 201–220.

[2] K. Hamdi, W. Zhang, and K. Letaief, Opportunistic spectrum sharing in cognitive MIMO wireless networks, *IEEE Trans. on Wireless Communications* **8** (2009) 4098–4109.

[3] J. Zhou, and J. Thompson, Single-antenna selection for MISO cognitive radio, *IET Semin. Cognitive Radio Software Defined Radios: Technol. Techn.* (2008) 1–5.

[4] H. Yin, and S. Alamouti, Parallel algorithm for path covering, OFDMA: A Broadband Wireless Access Technology, *IEEE, Sarnoff Symposium* (2006) 1–4.

[5] I. Akyildiz, W.Y. Lee, M. Vuran, and S. Mohanty, NeXt Generation/Dynamic Spectrum Access/Cognitive Radio Wireless Networks: A Survey, *Computer Networks (Elsevier) Journal* (2006).

[6] E.A. Gharavol, Y.-C. Liang, and K. Mouthaan, Robust downlink beamforming in multiuser MISO cognitive radio networks with imperfect channel-state information, *IEEE Trans. Veh. Technology* **56** (2010) 2852–2860.

[7] D. Hu, S. Mao, Y.T. Hou, and J.H. Reed, Scalable Video Multicast in Cognitive Radio Networks, *IEEE Journal on selected areas in Communications* **28** (2010) 334–344.

[8] M. Z. Bocus, J. P. Coon, C. N. Canagarajah, S.M.D. Armour, A. Doufexi, and J. P. McGeehan, Per-Subcarrier Antenna Selection for H.264 MGS/CGS Video Transmission Over Cognitive Radio Networks, *IEEE Trans. on Veh. Technology* **61** (2012) 1060–1072.

[9] Q. Ni, and Ch. Zarakovitis, Nash Bargaining Game Theoretic Scheduling for Joint Channel and Power Allocation in Cognitive Radio Systems, *IEEE Journal on selected areas in Communications* **30** (2012) 70–81.

[10] D. Ngo, C. Tellambura, and H. Nguyen, Resource Allocation for OFDM-based Cognitive Radio Multicast Networks, *IEEE Wireless Communications and Networking Conference* (2009) 1–6.

[11] C. Y. Wong, R.S. Cheng, K.B. Lataief, and R.D. Murch, Multiuser OFDM with adaptive subcarrier, bit and power allocation, *IEEE Journal on Selected Areas in Communications* **17** (1999) 1747–1758.

[12] H. Kushwaha, Y. Xing, R. Chandramouli, and H. Heffes, Reliable multimedia transmission over cognitive radio networks using fountain codes, *IEEE* **96** (2008) 155–165.

[13] H. Mansour, J.W. Huang, and V. Krishnamurthy, Multi-user scalable video transmission control in cognitive radio networks as a Markovian dynamic game, *48th IEEE CDC and 28th CCC* **8** (2009) 4735–4740.

[14] H. Mahmoud, T. Yucek, and H. Arslan, OFDM for Cognitive Radio: Merits and Challenges, *Wireless Communications, IEEE Wireless Communications* **16** (2009) 6–15.

[15] Q. Zhang, A. Kokkeler, and G. Smit, An Efficient FFT For OFDM Based Cognitive Radio On A Reconfigurable Architecture, *IEEE International Conference on Communications* (2007) 6522–6526.

[16] A. Sahai, N. Hoven, R. Tandra, Some fundamental limits in cognitive radio, *Allerton Conf. on Commun., Control and Computing* (2004).

[17] A. Ghasemi, E.S. Sousa, Collaborative spectrum sensing for opportunistic access in fading environment, *Proc. IEEE DySPAN 2005* (2005) 131–136.

[18] R. Zhang, and Y.-C. Liang, Exploiting Multi-Antennas for Opportunistic Spectrum Sharing in Cognitive Radio Networks, *IEEE Journal of Selected Topics in Signal Processing* (2008) 88–102.

[19] S. Pathak, and H. Sharma, Channel Estimation in OFDM Systems, *International Journal of Advanced Research in Computer Science and Software Engineering* **3** (2013) 312–327.

[20] J.G. Proakis, M. Salehi, Communication Systems Engineering(2nd Edition), Prentice Hall (2002).

[21] H. Schwarz, D. Marpe, and T. Wiegand, Overview of the Scalable Video Coding Extension of the H.264/AVC Standard, *IEEE Trans. on Circuits and Systems for Video Technology* **17** (2007) 1103–1120.

[22] H.-S. Huang, W.-H. Peng, and T. Chiang, Advances in the scalable amendment of H.264/AVC, *IEEE Communications Magazine* **45** (2007).

[23] Joint Scalable Video Model 9.19.14.

[24] G.-M. Su, Z. Han, M. Wu, and K.J. Ray Liu, A Scalable Multiuser Framework for Video over OFDM Networks: Fairness and Efficiency, *IEEE Trans. on Circuits and System for Video Technology* **16** (2006) 1217–1231.

[25] K.E. Parsopoulos, and M.N. Vrahatis, *Particle Swarm Optimization and Intelligence: Advances and Applications*, Information Science Publishing, 2010.

[26] R.C. Eberhart, and J. Kennedy, A new optimizer using particle swarm theory, *Proceedings Sixth Symposium on Micro Machine and Human Science* (1995) 39–43.

[27] B. Wang, Y. Wu, and K.J.R. Liu, Game theory for cognitive radio networks: An overview, *Computer Networks: The International Journal of Computer and Telecommunications Networking* **54** (2010) 2537–2561.

[28] K. Binmore, *Playing For Real: A text on Game Theory*, Oxford University Press, 2007 **56** (2010) 2852–2860.

[29] M. Clerc, and J. Kennedy, The particle swarm-explosion, stability and convergence in a multidimensional complex space, *IEEE Trans. Evol. Comput.* **6** (2002) 58-73.

[30] A. V. Katsenou, L. P. Kondi, and K. E. Parsopoulos, Resource management for wireless visual sensor networks based on individual video characteristics, *IEEE International Conference on Image Processing* (2011).

[31] K. Pandremmenou, L. P. Kondi, and K. E. Parsopoulos, Fairness issues in Resource allocation schemes for wireless visual sensors, *Visual Information Processing and Communication IV, SPIE-IS T Electronic Imaging* (2013).

[32] http://trace.eas.asu.edu/yuv/index.html

Short Vita

Alexandros Fragkoulis was born in Ioannina, Greece, in 1982. In 2006, he graduated from the Aristotle University of Thessaloniki, Greece, with a Diploma in Electrical and Computer Engineering, with specialization in Telecommunications. In 2011, he was admitted at the postgraduate program of Computer Science and Engineering department, University of Ioannina, Greece. In 2014, he completed successfully the program and received his MSc degree, with specialization in Technologies-Applications.